Arch Toxicol
DOI 10.1007/s00204-012-0824-4

REPRODUCTIVE TOXICOLOGY

Transient aberration of neuronal development in the hippocampal dentate gyrus after developmental exposure to brominated flame retardants in rats

Yukie Saegusa · Hitoshi Fujimoto · Gye-Hyeong Woo · Takumi Ohishi · Liyun Wang · Kunitoshi Mitsumori · Akiyoshi Nishikawa · Makoto Shibutani

Received: 29 September 2011 / Accepted: 27 February 2012

Abstract We immunohistochemically investigated the impact and reversibility of three brominated flame retardants (BFRs) known to be weak thyroid hormone disruptors on neuronal development in the hippocampal formation and apoptosis in the dentate subgranular zone. Pregnant Sprague–Dawley rats were exposed to 10, 100, or 1,000 ppm decabromodiphenyl ether (DBDE); 100, 1,000 or 10,000 ppm tetrabromobisphenol A (TBBPA) or 1,2,5,6,9,10-hexabromocyclododecane (HBCD) in the diet from gestational day 10 through to day 20 after delivery (weaning). On postnatal day (PND) 20, interneurons in the dentate hilus–expressing reelin increased with all chemicals, suggestive of aberration of neuronal migration. However, this increase had disappeared by PND 77. NeuN-positive mature neurons increased in the hilus on PND 77 with all chemicals. In the subgranular zone on PND 20, an increase in apoptotic bodies suggestive of impaired neurogenesis was observed after exposure to TBBPA or HBCD. The effects on neuronal development were detected at doses of ≥100 ppm DBDE; ≥1,000 ppm TBBPA; and at least at 10,000 ppm HBCD. On PND 20, the highest dose of DBDE and HBCD revealed mild fluctuations in the serum concentrations of thyroid-related hormones suggestive of weak developmental hypothyroidism, while TBBPA did not. Thus, DBDE and TBBPA may exert direct effect on neuronal development in the brain, but hypothyroidism may be operated for DBDE and HBCD at high doses. An excess of mature neurons in the hilus at later stages may be the signature of the developmental effects of BFRs. However, the effect itself was reversible.

Keywords Reelin · Brominated flame retardants · Hippocampal dentate gyrus · Hypothyroidism · Neurogenesis · Neuronal migration

Abbreviations

BFRs	Brominated flame retardants
BW	Body weight
CA1	Cornu ammonis 1
DBDE	Decabromodiphenyl ether
EphA5	Ephrin type A receptor 5
GABA	γ-Aminobutyric acid
GAD67	Glutamic acid decarboxylase 67
GD	Gestational day
HBCD	1,2,5,6,9,10-Hexabromocyclododecane
NeuN	Neuron-specific nuclear protein
PND	Postnatal day
SGZ	Subgranular zone
Tacr3	Tachykinin receptor 3

Electronic supplementary material The online version of this article (doi:10.1007/s00204-012-0824-4) contains supplementary material, which is available to authorized users.

Y. Saegusa · T. Ohishi · L. Wang · K. Mitsumori · M. Shibutani (✉)
Laboratory of Veterinary Pathology, Tokyo University of Agriculture and Technology, 3-5-8 Saiwai-cho, Fuchu-shi, Tokyo 183-8509, Japan
e-mail: mshibuta@cc.tuat.ac.jp

Y. Saegusa
Pathogenetic Veterinary Science, United Graduate School of Veterinary Sciences, Gifu University, 1-1 Yanagido, Gifu-shi, Gifu 501-1193, Japan

H. Fujimoto · G.-H. Woo · M. Shibutani
Division of Pathology, National Institute of Health Sciences, 1-18-1 Kamiyoga, Setagaya-ku, Tokyo 158-8501, Japan

A. Nishikawa
Biological Safety Research Center, National Institute of Health Sciences, 1-18-1 Kamiyoga, Setagaya-ku, Tokyo 158-8501, Japan

Published online: 14 March 2012

TBBPA	Tetrabromobisphenol A
TH	Thyroid hormone
T_3	Triiodothyronine
T_4	Thyroxine
TSH	Thyroid-stimulating hormone

Introduction

Thyroid hormones (THs) are essential for normal brain development in animals and humans. They regulate neuronal proliferation, migration, and differentiation in discrete regions of the brain during definitive time periods (Porterfield 2000). Experimentally, developmental hypothyroidism leads to growth retardation, neurological defects, and impaired performance in a variety of behavioral learning actions (Comer and Norton 1982; Akaike et al. 1991). Rat offspring exposed in utero to maternal antithyroid agents show impaired brain growth with neuronal mismigration and white matter hypoplasia involving limited axonal myelination and decreased oligodendroglial distribution (Lavado-Autric et al. 2003; Schoonover et al. 2004). The outcome of this type of impairment is permanent and is accompanied by apparent structural and functional abnormalities.

The dentate gyrus in the hippocampal formation is a unique structure that can continue neurogenesis during postnatal life and is a well-known target for developmental hypothyroidism (Zhang et al. 2009). By developmental hypothyroidism, we have recently detected an increase in reelin-expressing γ-aminobutyric acid (GABA)ergic interneurons showing immature phenotype in the dentate hilus that was sustained through to the adult stage, as well as increased apoptosis and decreased cell proliferation suggestive of impaired neurogenesis in the neuroblast-producing subgranular zone (SGZ; Saegusa et al. 2010b). Reelin is a secreted extracellular matrix glycoprotein that plays a critical role in neuronal migration and positioning during brain development (D'Arcangelo et al. 1997; Alvarez-Dolado et al. 1999). Also, it has been suggested that reelin release by GABAergic interneurons in adults could regulate the migration and maturation of newborn granular cells in the dentate granular cell layer (Lussier et al. 2009). Therefore, our observation of the sustained increase in reelin-producing immature GABAergic interneurons in the hilus suggests a compensatory regulation for neuronal mismigration that continues to the adult stage in relation with developmental hypothyroidism (Saegusa et al. 2010b). Altered reelin signaling has been reported in the dentate gyrus in some neurological diseases such as depression and epilepsy (Lussier et al. 2009; Gong et al. 2007).

In a study to establish a morphometric detection system of aberrant neuronal migration, we have shown fluctuations in the distribution of pyramidal neurons in the cornu ammonis 1 (CA1) of the hippocampus in a model for hypothyroidism induced by maternal administration of antithyroid agents in rats (Shibutani et al. 2009). Using this model, we also identified candidates for immunohistochemical molecular markers reflecting impaired neuronal development in the hippocampal formation, such as Ephrin type A receptor 5 (EphA5) and Tachykinin receptor (Tacr)-3, using microarray analysis (Saegusa et al. 2010a). EphA5 is a tyrosine kinase receptor that is particularly important in mediating neurodevelopmental events, such as neurogenesis, neuronal migration, and the plasticity (Numachi et al. 2007; Cooper et al. 2009). Tacr3 is a tachykinin peptide neurotransmitter/neuromodulator receptor predominantly expressed in neurons involving the hippocampus (Smith and Dawson 2008). It has been shown to play a role in the survival and function of dopaminergic neurons (Salthun-Lassalle et al. 2005). We have previously found an increase in both EphA5- and Tacr3-immunoreactive cells with strong intensities in the pyramidal cell layer or stratum oriens of the CA1 on weaning after developmental hypothyroidism, with a sustained increase in Tacr3-expressing cells through to the adult stage (Saegusa et al. 2010a).

Some environmental chemicals are thought to potentiate a TH–disrupting effect that may lead to abnormal brain development (Bansal and Zoeller 2008). Particularly, brominated flame retardants (BFRs), some of which are environmental contaminants used in plastics, textiles, electronic circuitry and other materials to prevent fires, are known to be the weak TH disruptors. Therefore, there is a growing concern regarding the developmental neurotoxicity of these chemicals (de Wit 2002; Rice et al. 2007). Decabromodiphenyl ether (DBDE), tetrabromobisphenol A (TBBPA), and 1,2,5,6,9,10-hexabromocyclododecane (HBCD) are three widely used BFRs (Birnbaum and Staskal 2004) that have been reported to cause neurobehavioral and auditory response effects by developmental exposure in mice and rats (Rice et al. 2007; Viberg et al. 2003, 2007; van der Ven et al. 2008; Lilienthal et al. 2008; Eriksson et al. 2006; Ema et al. 2008). These BFRs have shown weak antithyroid activities in some studies (Kitamura et al. 2005; Rice et al. 2007; Ema et al. 2008; Saegusa et al. 2009; Fujimoto et al. 2011). On the other hand, there are experimental studies to suggest direct effect on the developing brain by these BFRs (Nakajima et al. 2009; Ibhazehiebo et al. 2011a, b, c).

We have recently reported the effects of developmental exposure to DBDE, TBBPA, and HBCD on the migration of the hippocampal CA1 pyramidal cells and white matter

development by histomorphometric assessment using rats in association with thyroid parameters (Saegusa et al. 2009; Fujimoto et al. 2011). Our results suggested that maternal exposure to DBDE or HBCD through diet caused irreversible white matter hypoplasia at highest doses in offspring as examined in males, as well as the induction of mild developmental hypothyroidism as judged by fluctuations in the serum concentrations of thyroid-related hormones at the end of developmental exposure (Saegusa et al. 2009; Fujimoto et al. 2011; Online Resource 1, Table s1). However, no effect of BFR exposure could be detected on histologically observable neuronal migration. In the present study, we investigated the effects of these BFRs on neuronal development by analyzing cellular changes in the distribution of reelin in the dentate hilus and of EphA5 and Tacr3 in the CA1 region immediately after developmental exposure and at later stages for analysis of reversibility using the same study samples examined previously (Saegusa et al. 2009; Fujimoto et al. 2011). We also examined the effects on neurogenesis in the SGZ in terms of apoptosis at both time points.

Materials and methods

Chemicals and animals

Decabromodiphenyl ether (DBDE; CAS No. 1163–19–5, purity: >98%) was purchased from Wako Pure Chemical Industries, Ltd. (Osaka, Japan). Tetrabromobisphenol A (TBBPA; CAS No.79–94–7, purity: >98%) and 1,2,5,6,9,10-hexabromocyclododecane (HBCD; CAS No. 3194–55–6, purity: >95%) were purchased from Tokyo Kasei Kogyo Co., Ltd. (Tokyo, Japan). Pregnant Crj:CD® (SD)IGS rats were purchased from Charles River Japan Inc. (Yokohama, Japan) at gestational day (GD) 3 (appearance of vaginal plugs was designated as GD 0). Rats were housed individually in polycarbonate cages with wood chip bedding, maintained in an air-conditioned animal room (temperature 24 ± 1°C, relative humidity: 55 ± 5%) with a 12-h light/dark cycle and allowed ad libitum access to feed and tap water (Saegusa et al. 2009; Fujimoto et al. 2011). A soy-free diet (Oriental Yeast Co., Ltd., Tokyo, Japan) was chosen as the basal diet for the dams to eliminate possible phytoestrogen effects as described previously (Masutomi et al. 2003). All offspring consumed a regular CRF-1 basal diet (Oriental Yeast Co., Ltd.) and water ad libitum from postnatal day (PND) 20 onwards (PND 0 being the day of delivery). Although the formula is not public, CRF-1 contains soybean and alfalfa-derived proteins and oils including daidzin and genistin at concentrations of 87 and 102 ppm according to the supplier's analysis, and coumestrol of <3 ppm based on the content of lucerne meal in the diet (supplier's comment). The soy-free diet was prepared based on the formulation of the NIH-07 open formula rodent diet, in which soybean meal and soy oil were replaced with ground corn, ground wheat, wheat middlings and corn oil. Values for phytoestrogens in this diet were below the detection limit (0.5 ppm), except for coumestrol (3 ppm). Estrogen equivalents of phytoestrogens included in the CRF-1 and soy-free diet were roughly calculated as 0.91 and 0.06 ppm, respectively, for β-estradiol, based on the relative binding affinities in a rat endometrium-derived experimental model (Hopert et al. 1998). Nutritional standards did not differ between the soy-free diet and CRF-1 (supplier's analysis).

Animal experiments

Exposure studies to DBDE, HBCD, and TBBPA were individually performed, and dams were randomly divided into four groups including untreated controls (Saegusa et al. 2009; Fujimoto et al. 2011). The highest dose of each chemical was determined with a preliminary dose-finding study by estimating the dose range that causes changes in thyroid weights and histopathological findings of thyroid glands in dams, but does not affect pregnancy, implantation, or delivery. For DBDE, 8 dams per group were provided with the soy-free diet containing 0 (control), 10, 100, or 1,000 ppm of DBDE from GD 10 to day 20 after delivery. For TBBPA or HBCD, 8 dams per group in the TBBPA study and 10 dams per group in the HBCD study were provided with the soy-free diet containing 0 (control), 100, 1,000, or 10,000 ppm of the compound from GD 10 to day 20 after delivery. In all studies, litters were culled randomly on PND 2, leaving 4 male and 4 female offspring. On PND 20, 20 male and 20 female offspring (at least one male and one female per dam) per group were killed and subjected to prepubertal necropsy. Body and brain weights were measured for 10 male offspring at PND 20. The remaining animals were killed on PND 77 and subjected to adult stage necropsy. Body and brain weights were measured.

All animals used in the present study were killed by exsanguination from the abdominal aorta under deep anesthesia with ether. The protocols were reviewed in terms of animal welfare and approved by the Animal Care and Use Committee of the National Institute of Health Sciences, Japan.

As reported previously, no major treatment-related changes were observed in dams during gestation and lactation periods in all studies (Saegusa et al. 2009; Fujimoto et al. 2011; Online Resource 1, Table s2). At necropsy on day 20 after delivery, dose-unrelated increase in the relative thyroid weight was observed at 10 and 1,000 ppm in the DBDE study. In the TBBPA study, there were no

statistically significant changes in relative weight and histopathology of the thyroid on this time point. In the HBCD study, a significant increase in relative thyroid weights associated with significantly increased incidence and severity of diffuse thyroid follicular cell hypertrophy was observed at 10,000 ppm.

With regard to the body and organ weights of offspring as examined in males, no treatment-related changes in body and relative brain weights were observed on PND 20 in all studies (Fujimoto et al. 2011; Saegusa et al. 2009; Online Resource 1, Table s3). On PND 77, dose-unrelated increase in body weight and decrease in relative brain weights were observed at 10 and 100 ppm in the DBDE study, while relative thyroid weights were unchanged at any dose. In the TBBPA study, no treatment-related changes were observed in these parameters. In the HBCD study, a slight but significant dose-related increase was observed in relative thyroid weight from 1,000 ppm at this time point, while body and relative brain weights were unchanged.

Immunohistochemistry and Cresyl violet staining

For immunohistochemical studies, brains of male pups obtained at PND 20 or PND 77 were fixed in Bouin's solution at room temperature overnight. For analysis of PND 20 tissues, 5–6 animals (1 pup/litter) were examined per group including untreated controls in the DBDE study, 8 animals (1 pup/litter) were used per group in the TBBPA study, and 10 animals (1 pup/litter) per group in the HBCD study. For analysis of PND 77 tissues, 10 animals (1–2 pups/litter) were used from the untreated controls and the 10 ppm and 100 ppm DBDE exposure groups, and 11 (1–2 pups/litter) from the 1,000 ppm exposure group. In the TBBPA study, 10 animals (1–2 pups/litter) were used from the untreated controls and all exposure groups. In the HBCD study, 13 animals were used from the untreated controls, and 14 from the 100 ppm, 12 from the 1,000 ppm, and 14 from the 10,000 ppm exposure groups (1–2 pups/litter). Coronal slices were prepared from brains of PND 20 and PND 77 at the positions of −3.0 and −3.5 mm from the bregma, respectively.

Immunohistochemistry was performed on 3-μm brain tissue sections of animals killed at PND 20 and PND 77 with antibodies against reelin (clone G10, mouse IgG_1, 1:1,000; Novus Biologicals, Inc., Littleton, CO, United States), glutamic acid decarboxylase 67 (GAD67; clone 1G10.2, mouse IgG_{2a}, 1:50; Millipore Corporation Temecula, CA, United States), EphA5 (rabbit IgG, 1:50; Abcam, Cambridge, UK), and Tacr3 (rabbit polyclonal antibody, 1:3,000; Novus Biologicals, Inc.) as previously described (Saegusa et al. 2010a, b). Immunohistochemistry of neuron-specific nuclear protein (NeuN; clone A60, mouse IgG_1, 1:1,000; Millipore Corporation), which specifically detects postmitotic neurons, was performed on PND 77 brain sections (Saegusa et al. 2010b). Antigen retrieval treatment was not conducted for these antigens. Immunodetection was carried out using a VECTASTAIN® Elite ABC kit (Vector Laboratories Inc., Burlingame, CA, United States) with 3,3′-diaminobenzidine/H_2O_2 as the chromogen, as described previously (Saegusa et al. 2010a, b). The sections were then counterstained with hematoxylin and coverslipped for microscopic examination.

For evaluation of apoptosis in the hippocampal substructure, apoptotic bodies were detected by Cresyl violet staining as described by others (Nuñez and McCarthy 2004).

Morphometry of immunolocalized cells and apoptotic cells

Reelin-, NeuN-, or GAD67-positive cells distributed in the hilus of the dentate gyrus were bilaterally counted and averaged per mm^2 of hilar area (polymorphic layer) as described previously (Fig. 1; Saegusa et al. 2010b). EphA5- or Tacr3-immunoreactive cells distributed in the pyramidal cell layer or stratum oriens of the hippocampal CA1 region were bilaterally counted and normalized for

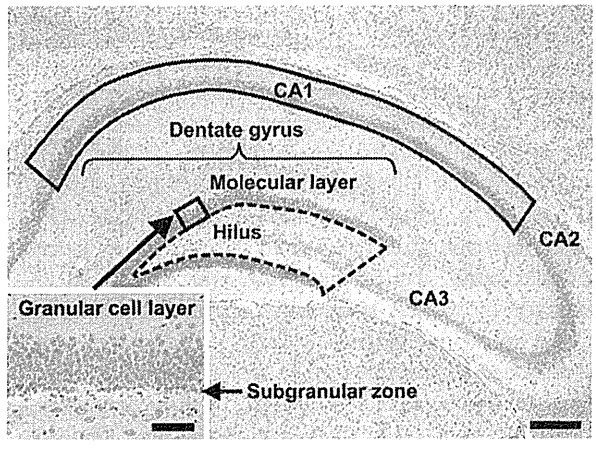

Fig. 1 Overview of the hippocampal formation of a male rat at PND 20 stained with hematoxylin and eosin. *Inset* shows a higher magnification of the granular cell layer and subgranular zone. *Bar* = 200 μm (*Inset*: 100 μm). Immunoreactive cells for reelin and GAD67 were counted in the hilus of the dentate gyrus, as enclosed by the *dotted line*, and averaged per area unit. Small-sized neurons in this area showed positive immunoreactivity with these antigens, but large-sized CA3 neurons distributed in this area were not immunoreactive. NeuN-immunoreactive cells were similarly counted and averaged per area unit, but CA3 neurons distributed in this area that were positive for NeuN were excluded from counting. The number of cells immunoreactive for EphA5 and Tacr3 in the area within the pyramidal cell layer and stratum oriens of the CA1 region, enclosed by a *solid line*, was normalized for the length of CA1 measured

the length of the CA1 region measured as previously described (Saegusa et al. 2010a). Apoptotic bodies detected by Cresyl violet staining were bilaterally counted and averaged per unit length of the SGZ as previously described (Saegusa et al. 2010b). For quantitative measurement of immunoreactive cells and apoptotic bodies, digital photomicrographs at 100-fold magnification were taken using a BX51 microscope (Olympus Optical Co., Ltd., Tokyo, Japan) attached to a DP70 Digital Camera System (Olympus Optical Co., Ltd.). Quantitative measurements were taken using the WinROOF image analysis software package (version 5.7, Mitani Corp., Fukui, Japan).

Statistical analysis

Numerical data were analyzed for homogeneity of variance using Bartlett's test. When the variance was homogeneous among the groups, a one-way analysis of variance was carried out. If significant differences were found, the mean value for each exposure group was compared with that of the controls using Dunnett's test. When the variance was heterogeneous based on Bartlett's test, the Kruskal–Wallis's *H* test was employed to check for differences among the groups. If significant differences appeared, a Dunnett-type rank-sum test was performed.

Results

Reelin-, NeuN-, and GAD67-immunoreactive cells in the hippocampal dentate hilus

The distribution of reelin-, NeuN-, and GAD67-immunoreactive cells in the hippocampal formation including the CA1–3 regions was similar to that described previously. Immunoreactive cells within the hilus of the dentate gyrus were predominantly interneurons (Saegusa et al. 2010b).

On PND 20, statistically significant dose-related increases in the number of reelin-immunoreactive cells were observed at 100 ppm and higher in the dentate hilus in both the DBDE and TBBPA studies (Fig. 2a). In the HBCD study, a statistically significant increase in the number of reelin-positive cells was observed at 1,000 ppm compared with the untreated controls on PND 20. However, the number at 10,000 ppm was not different from untreated controls. On PND 77, there were no effects of any of the BFRs on the number of reelin-positive cells in the hilus at any dose.

At PND 77, a weak but statistically significant increase in NeuN-immunoreactive cells was found in the hilus at 1,000 ppm in the DBDE study (Fig. 2b). In the TBBPA study, a slight dose-related increase in NeuN-positive cells was observed at 1,000 ppm and higher. In the HBCD study, a significant increase in NeuN-positive cells was observed at 10,000 ppm.

No changes were observed in the number of GAD67-immunoreactive cells in the highest dose groups compared with the untreated controls at both PND 20 and PND 77 in any of DBDE, TBBPA, and HBCD studies (Fig. 3).

EphA5- and Tacr3-immunoreactive cells in the hippocampal CA1 region

Both EphA5- and Tacr3-positive cells were sparse within the pyramidal cell layer or stratum oriens of the CA1 region, as shown in our previous study (Saegusa et al. 2010a).

With regard to EphA5-immunoreactivity, a significantly increased number of positive cells were observed only at 1,000 ppm on PND 20 in the DBDE study (Fig. 4a). There was no effect on the number of EphA5-positive cells in the TBBPA and HBCD studies at any dose at this time point. In the DBDE study, the number of EphA5-positive cells on PND 77 was unchanged at any dose, and the number of positive cells was low compared with PND 20.

With regard to Tacr3-immunoreactivity on PND 20, positive cells were mostly absent from the area lateral to the pyramidal cell layer of the CA1 region. There were no dose-related responses in any of DBDE, TBBPA, and HBCD studies (Fig. 4b).

Apoptotic cell indices in the SGZ

Few apoptotic bodies were found in the SGZ of the untreated controls in all studies at PND 20. In the DBDE study, no significant changes were observed at any dose at this time point. A slight but statistically significant increase was observed in the number of apoptotic bodies after exposure to 10,000 ppm TBBPA and 10,000 pm HBCD, as compared with their respective untreated controls (Fig. 5). However, on PND 77, we detected very few apoptotic bodies in any of the cases including the untreated controls without statistically significant differences in any of the DBDE, TBBPA, and HBCD studies (Fig. 5).

Discussion

In the present study, we found an increase in reelin-expressing interneurons in the dentate hilus of offspring of dams exposed to the middle and higher dose of DBDE and TBBPA or the middle dose of HBCD at the end of exposure on PND 20. We also observed an increase in apoptotic cells in the neuroblast-producing SGZ of the dentate gyrus after exposure to high doses of TBBPA and HBCD on this time point. Reelin functions on neuronal migration and

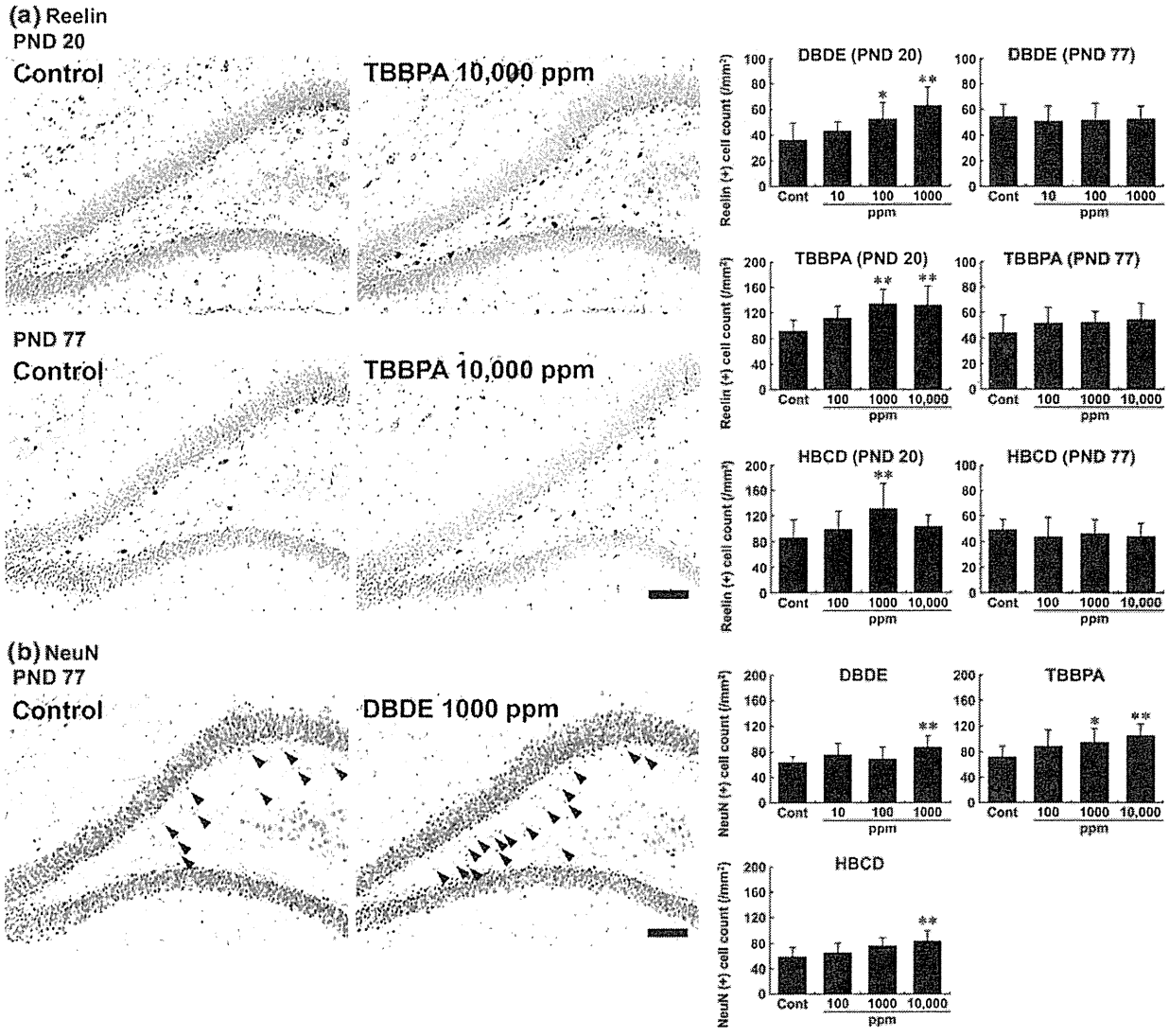

Fig. 2 Distribution of cells immunoreactive for reelin and NeuN in the hippocampal dentate gyrus in rat offspring after maternal exposure to DBDE, TBBPA, or HBCD. **a** Reelin-immunoreactive cells in the hilus of the dentate gyrus at PND 20 and PND 77. Reelin-positive cells with abundant cytoplasm show scattered distribution within the hilar region of the dentate gyrus. Note the higher number of reelin-positive cells in an animal exposed to 10,000 ppm TBBPA (*upper right*) compared with the control animal (*upper left*) on PND 20, while the number of reelin-positive cells in an animal in this group (*lower right*) at PND 77 was not different from the control animal (*lower left*). *Bar* = 100 μm. The graphs show the number of reelin-positive cells/unit area (mm^2) of the hilus of the bilateral hemispheres examined on both PND 20 and PND 77. Values were expressed as mean + SD. $N = 5$–14 in each group. $^*P < 0.05$, $^{**}P < 0.01$ versus controls (0 ppm) by Dunnett's test or Dunnett-type rank-sum test. **b** NeuN-immunoreactive cells as indicated with *arrowheads* at PND 77. NeuN-positive mature neurons are mainly distributed in the hilar area medial to the SGZ. Note the higher number of NeuN-positive cells in an animal exposed to 1,000 ppm DBDE (*right*) compared with the control animal (*left*). *Bar* = 100 μm. The graphs show the number of NeuN-positive cells/unit area (mm^2) of the hilus of the bilateral hemispheres on PND 77. Values were expressed as mean + SD. $N = 8$–10 in each group. $^*P < 0.05$, $^{**}P < 0.01$ versus controls (0 ppm) by Dunnett's test or Dunnett-type rank-sum test

positioning during brain development (D'Arcangelo et al. 1997; Alvarez-Dolado et al. 1999). Therefore, our observation that the increase in reelin-producing cells at the end of developmental exposure to BFRs might be a signature of a compensatory regulation mechanism for neuronal mismigration following impaired neurogenesis of the dentate granular cells. Similar results were found with the cases with developmental hypothyroidism in our previous study (Saegusa et al. 2010b).

Hoareau et al. (2006) reported that the transient prenatal disturbance of neurogenesis by treatment with methylazoxymethanol induces a long-term increase in the number of

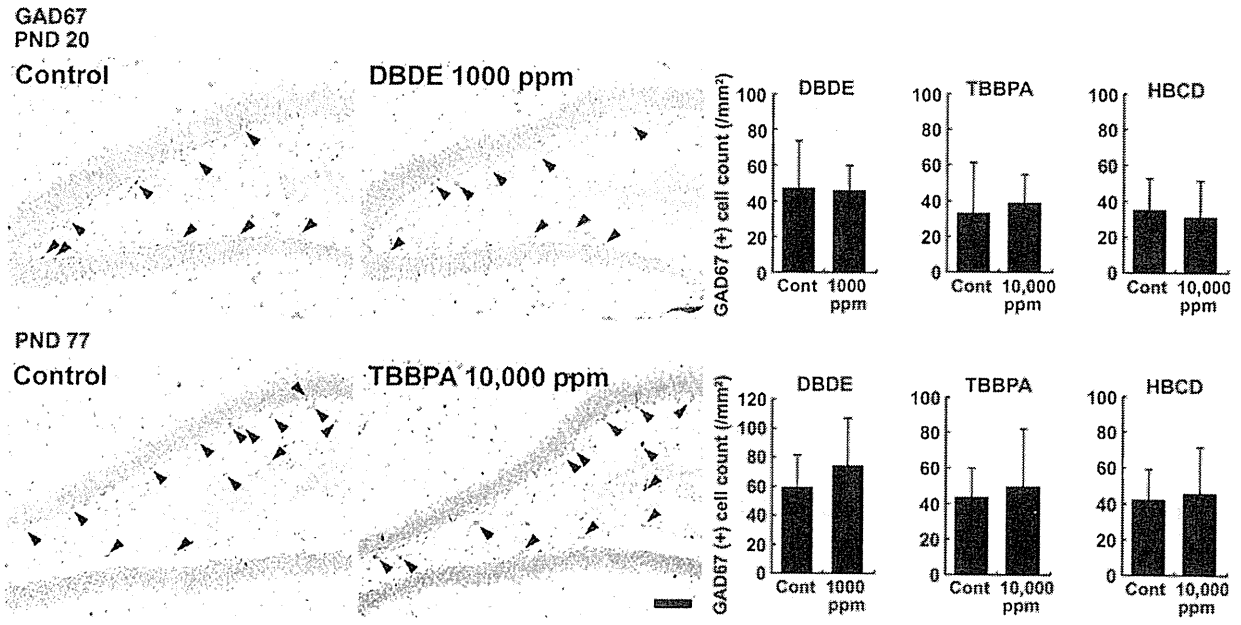

Fig. 3 Distribution of cells immunoreactive for GAD67 as indicated with *arrowheads* in the hilus of the dentate gyrus of rat offspring at PND 20 and PND 77 after maternal exposure to DBDE, TBBPA, or HBCD. *Bar* = 100 μm. The graphs show the number of GAD67-positive cells/unit area (mm^2) of the hilus of the bilateral hemispheres on both PND 20 and PND 77. Values were expressed as mean + SD. $N = 5$ in each group

reelin-expressing neurons in the hippocampus. In the present study, the number of reelin-producing cells in the hilus had returned to control levels on PND 77 in all experiments, which is different from the sustained increase after exposure to antithyroid agents we found previously (Saegusa et al. 2010b). Because reelin acts as a stop signal (Frotscher et al. 2003), the absence of excess population of reelin-expressing cells at later stages in the dentate hilus observed here could reflect a recovery to normal levels, to maintain the migration of the granular cells. Conversely, we found an increase in NeuN-positive mature neurons in the hilus after exposure to the middle and higher doses of TBBPA or the high dose of DBDE and HBCD on PND 77. We have also previously observed an increase in NeuN-positive mature neurons in addition to the sustained increase in reelin-expressing immature interneurons in the hilus by developmental hypothyroidism on PND 77 (Saegusa et al. 2010b), suggesting generation of an excess of mature neurons in the hilus as a sign of disruptive effect on neurogenesis and following neuronal migration during developmental exposure.

In the rodent dentate hilus, there are neurons other than GABAergic interneurons, in approximately equal numbers (Houser 2007). In the present study, we attempted to determine whether the increased number of NeuN-positive mature neurons were GABAergic interneurons. However, we did not observe fluctuations in the number of GAD67-positive cells at either PND 20 or PND 77 after BFR exposure. However, it has been reported that immunostaining with antibodies against GAD65 and GAD67 often produces inconsistencies between the antibodies, which makes it difficult to demonstrate an entire population of GABAergic interneurons (Houser 2007). This means that the cellular identity of NeuN-positive mature neurons in the present study remains unclear. Considering that reelin is an inducible molecule and its expression level can be modified during the disease process (Kundakovic et al. 2009; Stein et al. 2010), it may be reasonable to consider that the excess population of reelin-producing interneurons during the exposure to BFR halted their reelin production after the exposure ended, reflecting a recovery from the neuronal effects. While the biological significance should be assessed in further studies, the increase in mature neurons in the dentate gyrus at later stages may be the signature of the effects of chemical exposure during the developmental stages. As no changes were found in the distribution of CA1 pyramidal neurons and the number of reelin-expressing cells was reversible, the effects of BFRs on neuronal development is judged to be weak compared with those of antithyroid agents (Saegusa et al. 2010b).

Both thyrotoxic effects (Rice et al. 2007; Tseng et al. 2008) and developmental neurobehavioral effects (Rice et al. 2007) were reported in mice after exposure to DBDE, but no studies have been carried out in rats. In the present study, the offspring exposed to 1,000 ppm DBDE showed a slight decrease in serum triiodothyronine (T_3)

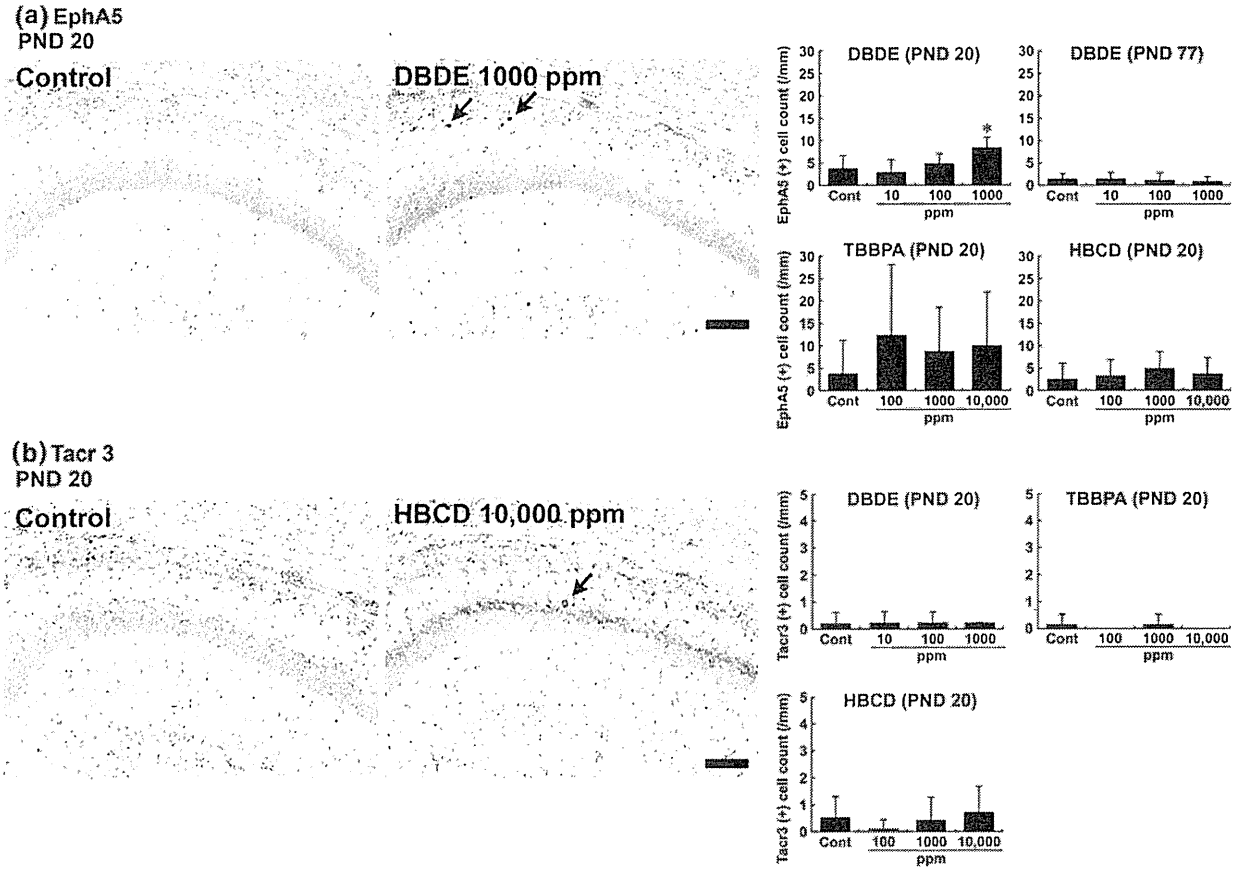

Fig. 4 Distribution of cells immunoreactive for EphA5 and Tacr3 in the hippocampal formation in rat offspring after maternal exposure to DBDE, TBBPA, or HBCD. **a** EphA5-immunoreactive cells located in the stratum oriens of the CA1 region on PND 20. *Bar* = 100 μm. Note a few EphA5-positive cells (*arrows*) in an animal exposed to 1,000 ppm DBDE (*right*) compared with no positive cells in a control animal (*left*). The graph shows the number of EphA5-positive cells/unit length (mm) of the CA1 region of the bilateral hemispheres on PND 20 or PND 77. Values were expressed as mean + SD. $N = 5$–10 in each group. $^*P < 0.05$ versus controls (0 ppm) by Dunnett's test or Dunnett-type rank-sum test. **b** Tacr3-immunoreactive cells located within the pyramidal cell layer and stratum oriens of the CA1 region on PND 20. *Bar* = 100 μm. Note one Tacr3-positive cell (*arrow*) in an animal exposed to 10,000 ppm HBCD (*right*). The graph shows the number of Tacr3-positive cells/unit length (mm) of the CA1 region of bilateral hemispheres on PND 20. Values were expressed as mean + SD. $N = 5$–10 in each group

concentrations accompanied with increase in the incidence of thyroid follicular cell hypertrophy on PND 20 (Fujimoto et al. 2011; Online Resource 1, Table s1). While we also observed non-significant increase in incidence of thyroid follicular cell hypertrophy in all exposure groups (Fujimoto et al. 2011), these results may suggest that DBDE at least at 1,000 ppm caused mild developmental hypothyroidism that was sustained until adult stage. Zhang et al. (2011) recently reported tissue distribution including the brain of DBDE and its debrominated metabolites in sucking rat pups after prenatal and/or postnatal exposure, suggesting a possibility of direct effect of DBDE on neuronal development. A relationship between the accumulation of DBDE in the brain and changes in spontaneous behavior was reported in mice after a single neonatal administration of DBDE (20.1 mg/kg body weight by oral gavage) on day 3 after birth, suggesting the possibility of a direct chemical effect on the neuronal development in the brain (Viberg et al. 2003); however, questions have been raised by others on the analytical methodology applied and data calculation (Vijverberg and van den Berg 2004; Goodman 2009). A similar neurobehavioral effects were observed in rats after a single administration of the same dose, but thyrotoxic effects were not examined (Viberg et al. 2007). In the present study, we observed an increase in reelin-expressing interneurons after exposure to DBDE of 100 ppm (7.0–22.8 mg/kg body weight/day) and higher on PND 20, suggesting primarily a direct effect of DBDE on neuronal development accompanied with hypothyroidism-related effect at 1,000 ppm. In another recent study, Ibhazehiebo et al. (2011a) reported disruption of TH-mediated transcription by DBDE in a reporter gene assay. Such effect

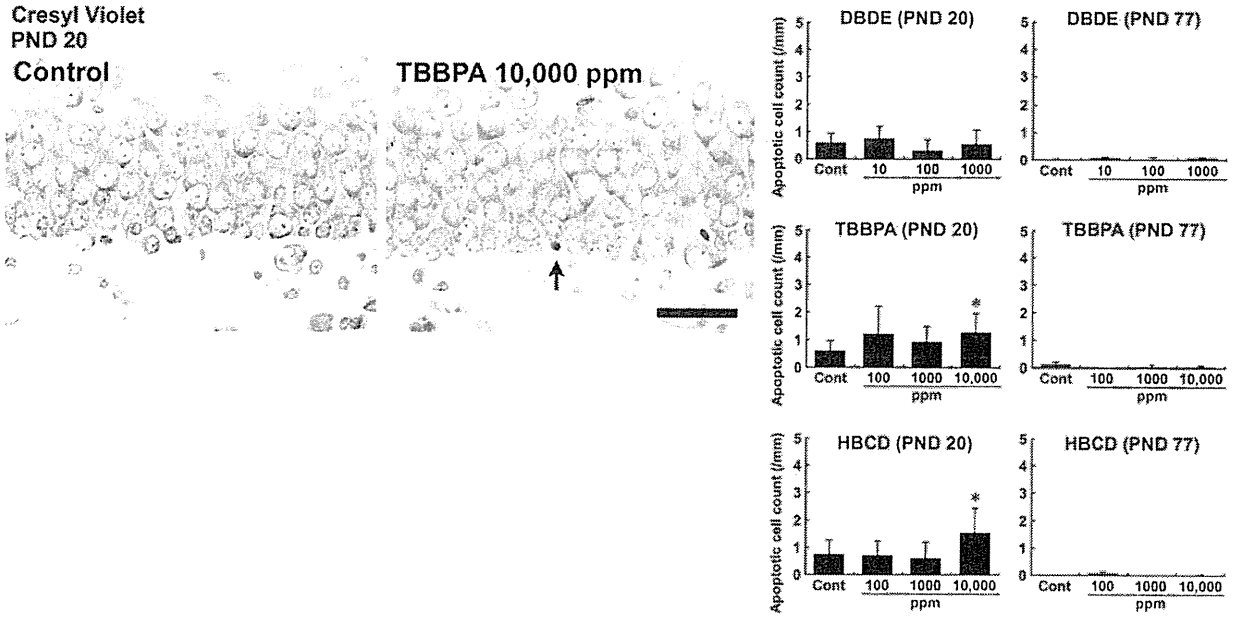

Fig. 5 Distribution of apoptotic cells in the dentate SGZ in rat offspring after maternal exposure to DBDE, TBBPA, or HBCD on both PND 20 and PND 77. Apoptotic cells were detected as apoptotic bodies with Cresyl violet staining. Note the apoptotic body (*arrow*) in an animal exposed to 10,000 ppm TBBPA (*right*) compared with the control animal without apoptotic bodies (*left*) at PND 20. *Bar* = 50 μm. The graph shows the number of apoptotic bodies/unit length (mm) of the SGZ of bilateral hemispheres at both PND 20 and PND 77. Values were expressed as mean + SD. $N = 5$–14 in each group. $^*P < 0.05$ versus controls (0 ppm) by Dunnett's test or Dunnett-type rank-sum test

appeared to be due to interference with the thyroid receptor-DNA binding domain. They also reported that DBDE was found to inhibit TH-induced dendrite arborization of Purkinje cells in vitro. These results suggest the potential of DBDE to suppress TH action in the brain. Interestingly, we also found development of mild white matter hypoplasia suggestive of hypothyroidism-related effect from the dose level at 100 ppm showing no significant alterations in the serum concentrations of thyroid-related hormones (Fujimoto et al. 2011).

TBBPA exposure during the gestation period has been shown to increase fetal plasma thyroid-stimulating hormone (TSH) concentration in rats, while circulating concentrations of T_3 and thyroxine (T_4) are unaltered in dams or their offspring (Meerts et al. 1999). In a recently published one-generation reproductive toxicity study of the effects of dietary TBBPA, auditory response effects, typically related to developmental hypothyroidism, were observed in offspring at the adult stage in association with serum TH changes (van der Ven et al. 2008). In the present study, however, no obvious thyrotoxic (including thyroid weight) changes were noted in the offspring except for a dose-unrelated decrease in serum T_3 concentrations at 100 and 1,000 ppm on PND 20 (Saegusa et al. 2009; Online Resource 1, Table s1). These results suggest that there was no obvious developmental hypothyroidism caused by TBBPA in the present study. With regard to the neurobehavioral effects of TBBPA, spatial learning was found to be impaired in the offspring of rats exposed to TBBPA at 250 mg/kg body weight/day (Hass and Wamberg 2002). Acute treatment of mice with TBBPA from the dose level as low as 0.1 mg/kg body weight revealed neurobehavioral effects and accumulation of TBBPA in the brain area (Nakajima et al. 2009), suggesting a possibility of direct effect of TBBPA on neuronal development. In the present study, we observed a dose-related increase in the number of reelin-expressing cells at 1,000 ppm (86.8–202.1 mg/kg body weight/day) and higher. Therefore, we suggest that TBBPA-induced brain changes may be a direct effect of TBBPA to the developing brain in the experimental conditions presented here. We have recently found a similar increase in reelin-expressing interneurons in the rat dentate hilus at the end of developmental exposure to acrylamide (Ogawa et al. 2011), a compound that has been proven to have no effects on gene expression, neurochemistry, hormone levels, or histopathology in the hypothalamus–pituitary–thyroid axis of rats (Bowyer et al. 2008).

HBCD is known to act as an inducer of cytochrome P450 (Germer et al. 2006) and uridine diphosphate-glucuronosyltransferase (van der Ven et al. 2006) in rats. This biological potential may be linked to the facilitation of TH metabolism by this enzyme to cause an increase in serum

TSH concentrations through the suppression of negative feedback by HBCD at 10,000 ppm on PND 20 in the present study. In the present study, a decrease in serum T_3 concentration and increase in serum TSH concentration on PND 20 after exposure to HBCD at 10,000 ppm suggest a development of mild hypothyroidism (Saegusa et al. 2009; Online Resource 1, Table s1). The effect was sustained until the adult stage, possibly because of the strong propensity for bioaccumulation as reported by others (Birnbaum and Staskal 2004; Chengelis 2001). As a hypothyroidism-related effect, HBCD reduced density of oligodendrocytes in the brain at 10,000 ppm (803.2–2,231.3 mg/kg body weight/day) in our previous study using the same study samples presented here (Saegusa et al. 2009). We also observed an increase in the number of NeuN-positive cells in the dentate hilus and increased apoptosis in the SGZ suggestive of the signature of impaired neuronal development after exposure to 10,000 ppm HBCD, although increased reelin-positive cells were only seen at the middle dose (1,000 ppm). Therefore, the effect of HBCD on neuronal development was observed at least at 10,000 ppm, similar to the effect on the number of oligodendrocytes in relation with developmental hypothyroidism. On the other hand, Yamada-Okabe et al. (2005) have shown a direct action of HBCD on TH receptors in a reporter gene assay. Disruption of TH-mediated neuronal development was also observed with HBCD (Ibhazehiebo et al. 2011b, c), as well as DBDE (Ibhazehiebo et al. 2011a), suggestive of the possible direct action on the developing brain.

Exposure to BFRs did not increase the number of cells expressing EphA5 or Tacr3 in the hippocampal CA1 region, which have been found to increase in number during developmental hypothyroidism (Saegusa et al. 2010a), except for a slight increase in EphA5-expressing cells on PND 20 after DBDE exposure. This suggests that these molecules could be considered to be less sensitive biomarkers for the detection of aberration in neuronal development such as neuronal mismigration compared with reelin.

In conclusion, we found that the BFRs examined here had developmental neuronal effect from doses of 100 ppm for DBDE, 1,000 ppm for TBBPA, and at least at 10,000 ppm for HBCD. A direct effect of DBDE and TBBPA on neuronal development may be considered under the present experimental conditions. However, the effect of hypothyroidism may also be operated at least at the highest dose of DBDE as well as that of HBCD. The effect of these BFRs on neurogenesis and following neuronal migration in the dentate gyrus may have occurred in the exposure period, while the biological significance of the increase in mature neuronal populations at the later stages should be further assessed. The results from this study suggest that reelin-expressing cells in the hippocampal dentate hilus may be used for the assessment of the effects of developmental neurotoxicants that can disrupt the migration and positioning of developing neurons following impairment of neurogenesis.

Acknowledgments We thank Miss Tomomi Morikawa for her technical assistance in conducting the animal studies. We also thank Mrs. Shigeko Suzuki for her technical assistance in preparing the histological specimens. This work was supported in part by Health and Labour Sciences Research Grants (Research on Risk of Chemical Substances) from the Ministry of Health, Labour and Welfare of Japan. All authors disclose that there are no conflicts of interest that could inappropriately influence the outcome of the present study.

References

Akaike M, Kato N, Ohno H, Kobayashi T (1991) Hyperactivity and spatial maze learning impairment of adult rats with temporary neonatal hypothyroidism. Neurotoxicol Teratol 13:317–322

Alvarez-Dolado M, Ruiz M, Del Río JA, Alcántara S, Burgaya F, Sheldon M, Nakajima K, Bernal J, Howell BW, Curran T, Soriano E, Muñoz A (1999) Thyroid hormone regulates reelin and dab1 expression during brain development. J Neurosci 19:6979–6993

Bansal R, Zoeller RT (2008) Polychlorinated biphenyls (Aroclor 1254) do not uniformly produce agonist actions on thyroid hormone responses in the developing rat brain. Endocrinology 149:4001–4008

Birnbaum LS, Staskal DF (2004) Brominated flame retardants: cause for concern? Environ Health Perspect 112:9–17

Bowyer JF, Latendresse JR, Delongchamp RR, Muskhelishvili L, Warbritton AR, Thomas M, Tareke E, McDaniel LP, Doerge DR (2008) The effects of subchronic acrylamide exposure on gene expression, neurochemistry, hormones, and histopathology in the hypothalamus-pituitary-thyroid axis of male Fischer 344 rats. Toxicol Appl Pharmacol 230:208–215

Chengelis CP (2001) A 90-day oral (gavage) toxicity study of HBCD in rats. WIL-186012. Brominated Flame Retardant Industry Panel. Chemical Manufacturers Association, Arlington, VA

Comer CP, Norton S (1982) Effects of perinatal methimazole exposure on a developmental test battery for neurobehavioral toxicity in rats. Toxicol Appl Pharmacol 63:133–141

Cooper MA, Crockett DP, Nowakowski RS, Gale NW, Zhou R (2009) Distribution of EphA5 receptor protein in the developing and adult mouse nervous system. J Comp Neurol 514:310–328

D'Arcangelo G, Nakajima K, Miyata T, Ogawa M, Mikoshiba K, Curran T (1997) Reelin is a secreted glycoprotein recognized by the CR-50 monoclonal antibody. J Neurosci 17:23–31

de Wit CA (2002) An overview of brominated flame retardants in the environment. Chemosphere 46:583–624

Ema M, Fujii S, Hirata-Koizumi M, Matsumoto M (2008) Two-generation reproductive toxicity study of the flame retardant hexabromocyclododecane in rats. Reprod Toxicol 25:335–351

Eriksson P, Fischer C, Wallin M, Jakobsson E, Fredriksson A (2006) Impaired behaviour, learning and memory, in adult mice neonatally exposed to hexabromocyclododecane (HBCDD). Environ Toxicol Pharmacol 21:317–322

Frotscher M, Haas CA, Förster E (2003) Reelin controls granule cell migration in the dentate gyrus by acting on the radial glial scaffold. Cereb Cortex 13:634–640

Fujimoto H, Woo GH, Inoue K, Takahashi M, Hirose M, Nishikawa A, Shibutani M (2011) Impaired oligodendroglial development by decabromodiphenyl ether in rat offspring after maternal exposure from mid-gestation through lactation. Reprod Toxicol 31:86–94

Germer S, Piersma AH, van der Ven L, Kamyschnikow A, Fery Y, Schmitz HJ, Schrenk D (2006) Subacute effects of the brominated flame retardants hexabromocyclododecane and tetrabromobisphenol A on hepatic cytochrome P450 levels in rats. Toxicology 218:229–236

Gong C, Wang TW, Huang HS, Parent JM (2007) Reelin regulates neuronal progenitor migration in intact and epileptic hippocampus. J Neurosci 27:1803–1811

Goodman JE (2009) Neurodevelopmental effects of decabromodiphenyl ether (BDE-209) and implications for the reference dose. Regul Toxicol Pharmacol 54:91–104

Hass U, Wamberg C (2002) Developmental neurotoxicity study of the brominated flame retardant tetrabromobisphenol A in rats. Reprod Toxicol 16:412 Abstract for 30th conference of the European teratology society, Hanover, 7th–11th September 2002

Hoareau C, Hazane F, Le Pen G, Krebs MO (2006) Postnatal effect of embryonic neurogenesis disturbance on reelin level in organotypic cultures of rat hippocampus. Brain Res 1097:43–51

Hopert AC, Beyer A, Frank K, Strunck E, Wunsche W, Vollmer G (1998) Characterization of estrogenicity of phytoestrogens in an endometrial-derived experimental model. Environ Health Perspect 106:581–586

Houser CR (2007) Interneurons of the dentate gyrus: an overview of cell types, terminal fields and neurochemical identity. Prog Brain Res 163:217–232

Ibhazehiebo K, Iwasaki T, Kimura-Kuroda J, Miyazaki W, Shimokawa N, Koibuchi N (2011a) Disruption of thyroid hormone receptor-mediated transcription and thyroid hormone-induced Purkinje cell dendrite arborization by polybrominated diphenyl ethers. Environ Health Perspect 119:168–175

Ibhazehiebo K, Iwasaki T, Xu M, Shimokawa N, Koibuchi N (2011b) Brain-derived neurotrophic factor (BDNF) ameliorates the suppression of thyroid hormone-induced granule cell neurite extension by hexabromocyclododecane (HBCD). Neurosci Lett 493:1–7

Ibhazehiebo K, Iwasaki T, Shimokawa N, Koibuchi N (2011c) 1,2,5,6,9,10-αHexabromocyclododecane (HBCD) impairs thyroid hormone-induced dendrite arborization of Purkinje cells and suppresses thyroid hormone receptor-mediated transcription. Cerebellum 10:22–31

Kitamura S, Kato T, Iida M, Jinno N, Suzuki T, Ohta S, Fujimoto N, Hanada H, Kashiwagi K, Kashiwagi A (2005) Anti-thyroid hormonal activity of tetrabromobisphenol A, a flame retardant, and related compounds: affinity to the mammalian thyroid hormone receptor, and effect on tadpole metamorphosis. Life Sci 76:1589–1601

Kundakovic M, Chen Y, Guidotti A, Grayson DR (2009) The reelin and GAD67 promoters are activated by epigenetic drugs that facilitate the disruption of local repressor complexes. Mol Pharmacol 75:342–354

Lavado-Autric R, Ausó E, García-Velasco JV, Arufe Mdel C, Escobar del Rey F, Berbel P, Morreale de Escobar G (2003) Early maternal hypothyroxinemia alters histogenesis and cerebral cortex cytoarchitecture of the progeny. J Clin Invest 111:1073–1082

Lilienthal H, Verwer CM, van der Ven LT, Piersma AH, Vos JG (2008) Exposure to tetrabromobisphenol A (TBBPA) in Wistar rats: neurobehavioral effects in offspring from a one-generation reproduction study. Toxicology 246:45–54

Lussier AL, Caruncho HJ, Kalynchuk LE (2009) Repeated exposure to corticosterone, but not restraint, decreases the number of reelin-positive cells in the adult rat hippocampus. Neurosci Lett 460:170–174

Masutomi N, Shibutani M, Takagi H, Uneyama C, Takahashi N, Hirose M (2003) Impact of dietary exposure to methoxychlor, genistein, or diisononyl phthalate during the perinatal period on the development of the rat endocrine/reproductive systems in later life. Toxicology 192:149–170

Meerts IATM, Assink Y, Cenijn PH, Weijers BM, van den Berg JHJ, Bergman Å, Koeman JH, Brouwer A (1999) Distribution of the flame retardant tetrabromobisphenol A in pregnant and fetal rats and effect on thyroid hormone homeostasis. Organohalogen Compd 40:375–378

Nakajima A, Saigusa D, Tetsu N, Yamakuni T, Tomioka Y, Hishinuma T (2009) Neurobehavioral effects of tetrabromobisphenol A, a brominated flame retardant, in mice. Toxicol Lett 189:78–83

Numachi Y, Yoshida S, Yamashita M, Fujiyama K, Toda S, Matsuoka H, Kajii Y, Nishikawa T (2007) Altered EphA5 mRNA expression in rat brain with a single methamphetamine treatment. Neurosci Lett 424:116–121

Nuñez JL, McCarthy MM (2004) Cell death in the rat hippocampus in a model of prenatal brain injury: time course and expression of death-related proteins. Neuroscience 129:393–402

Ogawa B, Ohishi T, Wang L, Takahashi M, Taniai E, Hayashi H, Mitsumori K, Shibutani M (2011) Disruptive neuronal development by acrylamide in the hippocampal dentate hilus after developmental exposure in rats. Arch Toxicol 85:987–994

Porterfield SP (2000) Thyroidal dysfunction and environmental chemicals—potential impact on brain development. Environ Health Perspect 108(Suppl 3):433–438

Rice DC, Reeve EA, Herlihy A, Zoeller RT, Thompson WD, Markowski VP (2007) Developmental delays and locomotor activity in the C57BL6/J mouse following neonatal exposure to the fully-brominated PBDE, decabromodiphenyl ether. Neurotoxicol Teratol 29:511–520

Saegusa Y, Fujimoto H, Woo GH, Inoue K, Takahashi M, Mitsumori K, Hirose M, Nishikawa A, Shibutani M (2009) Developmental toxicity of brominated flame retardants, tetrabromobisphenol A and 1,2,5,6,9,10-hexabromocyclododecane, in rat offspring after maternal exposure from mid-gestation through lactation. Reprod Toxicol 28:456–467

Saegusa Y, Woo G-H, Fujimoto H, Inoue K, Takahashi M, Hirose M, Igarashi K, Kanno J, Mitsumori K, Nishikawa A, Shibutani M (2010a) Gene expression profiling and cellular distribution of molecules with altered expression in the hippocampal CA1 region after developmental exposure to anti-thyroid agents in rats. J Vet Med Sci 72:187–195

Saegusa Y, Woo G-H, Fujimoto H, Kemmochi S, Shimamoto K, Hirose M, Mitsumori K, Nishikawa A, Shibutani M (2010b) Sustained production of Reelin-expressing interneurons in the hippocampal dentate hilus after developmental exposure to anti-thyroid agents in rats. Reprod Toxicol 29:407–414

Salthun-Lassalle B, Traver S, Hirsch EC, Michel PP (2005) Substance P, neurokinins A and B, and synthetic tachykinin peptides protect mesencephalic dopaminergic neurons in culture via an activity-dependent mechanism. Mol Pharmacol 68:1214–1224

Schoonover CM, Seibel MM, Jolson DM, Stack MJ, Rahman RJ, Jones SA, Mariash CN, Anderson GW (2004) Thyroid hormone regulates oligodendrocyte accumulation in developing rat brain white matter tracts. Endocrinology 145:5013–5020

Shibutani M, Woo G-H, Fujimoto H, Saegusa Y, Takahashi M, Inoue K, Hirose M, Nishikawa A (2009) Assessment of developmental effects of hypothyroidism in rats from in utero and lactation exposure to anti-thyroid agents. Reprod Toxicol 28:297–307

Smith PW, Dawson LA (2008) Neurokinin 3 (NK3) receptor modulators for the treatment of psychiatric disorders. Recent Pat CNS Drug Discov 3:1–15

Stein T, Cosimo E, Yu X, Smith PR, Simon R, Cottrell L, Pringle MA, Bell AK, Lattanzio L, Sauter G, Lo Nigro C, Crook T, Machesk LM, Gusterson BA (2010) Loss of reelin expression in breast cancer is epigenetically controlled and associated with poor prognosis. Am J Pathol 177:2323–2333

Tseng LH, Li MH, Tsai SS, Lee CW, Pan MH, Yao WJ, Hsu PC (2008) Developmental exposure to decabromodiphenyl ether (PBDE 209): effects on thyroid hormone and hepatic enzyme activity in male mouse offspring. Chemosphere 70:640–647

van der Ven LT, Verhoef A, van de Kuil T, Slob W, Leonards PE, Visser TJ, Hamers T, Herlin M, Håkansson H, Olausson H, Piersma AH, Vos JG (2006) A 28-day oral dose toxicity study enhanced to detect endocrine effects of hexabromocyclododecane in Wistar rats. Toxicol Sci 94:281–292

van der Ven LT, Van de Kuil T, Verhoef A, Verwer CM, Lilienthal H, Leonards PE, Schauer UM, Cantón RF, Litens S, De Jong FH, Visser TJ, Dekant W, Stern N, Håkansson H, Slob W, Van den Berg M, Vos JG, Piersma AH (2008) Endocrine effects of tetrabromobisphenol-A (TBBPA) in Wistar rats as tested in a one-generation reproduction study and a subacute toxicity study. Toxicology 245:76–89

Viberg H, Fredriksson A, Jakobsson E, Orn U, Eriksson P (2003) Neurobehavioral derangements in adult mice receiving decabrominated diphenyl ether (PBDE 209) during a defined period of neonatal brain development. Toxicol Sci 76:112–120

Viberg H, Fredriksson A, Eriksson P (2007) Changes in spontaneous behaviour and altered response to nicotine in the adult rat, after neonatal exposure to the brominated flame retardant, decabrominated diphenyl ether (PBDE 209). Neurotoxicology 28:136–142

Vijverberg HP, van den Berg M (2004) Re: Viberg H et al. (2003) Neurobehavioral derangements in adult mice receiving decabrominated diphenyl ether (PBDE 209) during a defined period of neonatal brain development. Toxicol Sci 76, 112–120. Toxicol Sci 79:205–206

Yamada-Okabe T, Sakai H, Kashima Y, Yamada-Okabe H (2005) Modulation at a cellular level of the thyroid hormone receptor-mediated gene expression by 1,2,5,6,9,10-hexabromocyclododecane (HBCD), 4,4′-diiodobiphenyl (DIB), and nitrofen (NIP). Toxicol Lett 155:127–133

Zhang L, Blomgren K, Kuhn HG, Cooper-Kuhn CM (2009) Effects of postnatal thyroid hormone deficiency on neurogenesis in the juvenile and adult rat. Neurobiol Dis 34:366–374

Zhang W, Cai Y, Sheng G, Chen D, Fu J (2011) Tissue distribution of decabrominated diphenyl ether (BDE-209) and its metabolites in sucking rat pups after prenatal and/or postnatal exposure. Toxicology 283:49–54

TOXICOLOGICAL SCIENCES 127(2), 508–521 (2012)
doi:10.1093/toxsci/kfs110
Advance Access publication March 9, 2012

Developmental Exposure to Manganese Chloride Induces Sustained Aberration of Neurogenesis in the Hippocampal Dentate Gyrus of Mice

Liyun Wang,* Takumi Ohishi,* Ayako Shiraki,* Reiko Morita,*,† Hirotoshi Akane,*,† Yoshiaki Ikarashi,‡ Kunitoshi Mitsumori,* and Makoto Shibutani*,[1]

*Laboratory of Veterinary Pathology, Tokyo University of Agriculture and Technology, Fuchu-shi, Tokyo 183-8509, Japan; †Pathogenetic Veterinary Science, United Graduate School of Veterinary Sciences, Gifu University, Gifu-shi, Gifu 501-1193, Japan; and ‡Division of Environmental Chemistry, National Institute of Health Sciences, Setagaya-ku, Tokyo 158-8501, Japan

[1]To whom correspondence should be addressed at Laboratory of Veterinary Pathology, Tokyo University of Agriculture and Technology, 3-5-8 Saiwai-cho, Fuchu-shi, Tokyo 183-8509, Japan. Fax: +81-42-367-5771. E-mail: mshibuta@cc.tuat.ac.jp.

Received January 19, 2012; accepted March 5, 2012

The effect of exogenously administered manganese (Mn) on developmental neurogenesis in the hippocampal dentate gyrus was examined in male mice after maternal exposure to $MnCl_2$ (0, 32, 160, or 800 ppm as Mn in diet) from gestational day 10 to day 21 after delivery on weaning. Immunohistochemistry was performed to monitor neurogenesis and interneuron subpopulations on postnatal days (PNDs) 21 and 77 (adult stage). Reelin-synthesizing γ-aminobutyric acid (GABA)ergic interneurons increased in the hilus with ≥ 160 ppm on weaning to sustain to PND 77 at 800 ppm. Apoptosis in the neuroblast-producing subgranular zone increased with 800 ppm and TUC4-expressing immature granule cells decreased with 800 ppm on weaning, whereas at the adult stage, immature granule cells increased. On PND 21, transcript levels increased with *Reln* and its receptor gene *Lrp8* and decreased with *Dpysl3* coding TUC4 in the dentate gyrus, confirming immunohistochemical results. Double immunohistochemistry revealed a sustained increase of reelin-expressing and NeuN-lacking or weakly positive immature interneurons and NeuN-expressing mature neurons in the hilus through to the adult stage as examined at 800 ppm. Brain Mn concentrations increased at both PNDs 21 and 77 in all $MnCl_2$-exposed groups. These results suggest that Mn targets immature granule cells causing apoptosis and neuronal mismigration. Sustained increases in immature reelin-synthesizing GABAergic interneurons may represent continued aberration in neurogenesis and following migration to cause an excessive response for overproduction of immature granule cells through to the adult stage. Sustained high concentration of Mn in the brain may be responsible for these changes.

Key Words: **manganese chloride ($MnCl_2$); hippocampal dentate gyrus; γ-aminobutyric acid (GABA)ergic interneurons; neurogenesis; reelin.**

Manganese (Mn) is a trace essential element necessary for immune function, regulation of blood sugar, cellular energy, reproduction, digestion and bone growth, which also aids in the defense against free radicals (Aschner and Aschner, 2005). Excess Mn can exert serious neurotoxic effects on both humans and experimental animals (Dobson *et al.*, 2004). Exposure of mature animals and humans to Mn produces neurological disorders, also known as manganism, with symptoms similar to those of Parkinsonism (Soldin and Aschner, 2007). Experimentally, neuronal death of the nigrostriatal dopaminergic system is a typical histological feature of manganism (Kitazawa *et al.*, 2005). Estimated safe and adequate daily dietary intake (ESADDI) of Mn has been estimated to be approximately 0.6 mg/day at 7–12 months of age, 1.2 mg/day at 1–3 years of age, 1.5 mg/day at 4–8 years of age and 2–5 mg/day for adults (Aschner and Aschner, 2005). On the other hand, ESADDI for newborns has been estimated to be 0.003 mg/day, less than that for adults or children (Aschner and Aschner, 2005). Several reports have documented that neonates are at an increased risk of Mn-induced neurotoxicity compared with adults due to their ability to achieve higher brain Mn levels and altered brain dopamine concentrations following Mn exposure (Chandra and Shukla, 1978; Dorman *et al.*, 2000; Kontur and Fechter, 1988). However, the risk of Mn-induced neurotoxicity during brain development, both pre- and postnatally, has received relatively little attention.

The hippocampal dentate gyrus, a unique structure that can continue neurogenesis during postnatal life, is crucial for higher brain functions such as learning, memory, and motivation (Montaron *et al.*, 2004). Postnatal neurogenesis (so-called adult neurogenesis) occurs in the neuroblast-producing subgranular zone (SGZ) of the dentate gyrus from type 1 progenitor cells and produces intermediate generations in the order of type 2a, type 2b, and type 3 cells in the SGZ. The type 3 cells undergo final mitosis to differentiate into immature granule cells and then to mature granule cells (Hodge *et al.*, 2008). In addition, within the dentate gyrus, γ-aminobutyric acid (GABA)ergic interneurons play a role in

the neuronal development and maintenance of granule cells. Reelin, an extracellular matrix glycoprotein, is expressed in these interneurons and aids in neuronal migration and ensures correct positioning (Ramos-Moreno *et al.*, 2006). Altered reelin-expression in the dentate gyrus has been reported to be a cause of some neurological diseases, such as depression and epilepsy (Gong *et al.*, 2007; Lussier *et al.*, 2009). Experimentally, developmental hypothyroidism leads to impaired neuronal migration as well as white matter hypoplasia involving limited axonal myelination and oligodendrocytic accumulation (Goodman and Gilbert, 2007; Lavado-Autric *et al.*, 2003; Schoonover *et al.*, 2004). We recently found sustained aberrant increases in immature GABAergic interneurons synthesizing reelin in the hilus of the dentate gyrus until the adult stage following developmental exposure to antithyroid agents, suggestive of the reflection of disrupted neuronal migration and positioning by these reagents (Saegusa *et al.*, 2010).

Experimental Mn exposure results in a high concentration of Mn in the dentate gyrus in neonatal rats (Takeda *et al.*, 1999) and has been shown to induce neurological, cognitive, and neuropsychological effects in children (Khan *et al.*, 2011); however, histopathological evidence of the impaired brain development by excess exposure to Mn is not clear. Because neonates are at an increased risk of Mn-induced neurotoxicity, a dose-response study of developmental neurotoxicity of Mn employing brain development parameters should be conducted. In the present study, to elucidate whether exogenously administered Mn targets developing neurons causing permanent disruption of neuronal differentiation, we examined neurogenesis in terms of cell proliferation, apoptosis, and differentiation in the dentate gyrus using mice following developmental $MnCl_2$ exposure. We also analyzed distribution changes of interneurons expressing reelin or glutamic acid decarboxylase (GAD) 67 in the dentate hilus. At the end of exposure at the weaning and adult stage, serum concentrations of thyroid-related hormones and brain concentrations of Mn were also analyzed. Because lactational Mn exposure has been shown to alter the iron (Fe) status of offspring in an inverse fashion (Garcia *et al.*, 2006), brain Fe concentrations were also measured.

MATERIALS AND METHODS

Chemicals and Animals

Manganese chloride hydrate ($MnCl_2 \cdot xH_2O$; CAS No. 73913-06-1) containing 27.8% Mn was purchased from Sigma Chemical Co (St Louis, MO). A total of 60 pregnant Slc:ICR mice were purchased from Japan SLC Inc. (Hamamatsu, Japan) at gestation day (GD) 1 (appearance of vaginal plugs was designated as GD 0). Animals were housed individually in polycarbonate cages with wood chip bedding, maintained in an air-conditioned animal room (temperature: 24 ± 1°C; relative humidity: 55 ± 5%) with a 12-h light/dark cycle and allowed access to food and tap water (Mn concentration: 0.000 mg/l) *ad libitum*. A regular MF basal diet (Oriental Yeast Co. Ltd., Tokyo, Japan) (Mn concentration 4.84 mg/100 g basal diet) and water were given *ad libitum* throughout the experimental period. All offspring consumed a regular MF basal diet and water *ad libitum* from postnatal day (PND) 21 onwards.

Experimental Design

All procedures of this study were conducted in compliance with the "Guidelines for Proper Conduct of Animal Experiments" (Science Council of Japan, June 1, 2006) and according to the protocol approved by the Animal Care and Use Committee of the Tokyo University of Agriculture and Technology.

Experiment 1. Maternal animals were randomly divided into four groups including untreated controls (Fig. 1). Fifteen dams per group were treated with 0, 32, 160, or 800 ppm of Mn in the form of $MnCl_2 \cdot xH_2O$ mixed in the powdered basal diet from GD 10 to PND 21 (PND 0: the day of delivery). This exposure period was determined because the formation of hippocampus starts from GD 11 and neurogenesis in the SGZ is active during postnatal period from PNDs 3 to 14 in mice (Reznikov, 1991). At PND 4, the 10 dams that delivered more than eight male offspring per group were selected to cull litters randomly, leaving eight male and two female offspring. Remaining dams were sacrificed under deep ether anesthesia, and the remaining offspring were sacrificed by rapid decapitation under ether anesthesia. At PND 21, 10 dams and 30 male and 20 female offspring (three male and two female offspring per dam) per group were subjected to prepubertal necropsy. The remaining male offspring were maintained until PND 77. At PND 77, all pups were subjected to adult stage autopsy. The body weights (BWs) and food consumptions of dams and pups were determined every 3–7 days. Mortality of pups was examined daily after birth (PND 2) until PND 77.

On PNDs 21 and 77, animals were weighed and sacrificed by exsanguination from the abdominal aorta under deep anesthesia with ether. Dams were examined for uterine implantation sites at autopsy on weaning. Brain, liver, and kidneys were collected at autopsy in 10 male and 10 female offspring per group. Because neurogenesis is influenced by circulating levels of steroid hormones during the estrous cycle (Pawluski *et al.*, 2009), male offspring were selected for immunohistochemical assays, and brains from 10 males per group (one male per dam) were prepared for this purpose. Brains from 10 male offspring per group and six dams per group were subjected to estimation of Mn and Fe concentrations in the cerebellum. Remaining brains from other offspring were used for other experimental purposes.

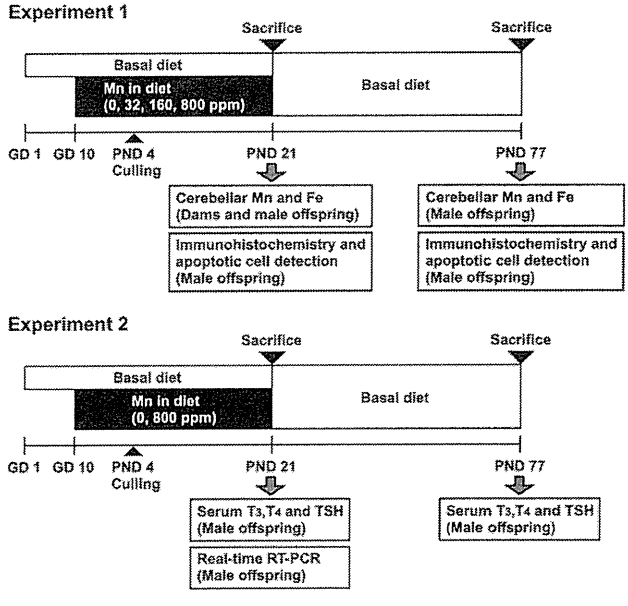

FIG. 1. Experimental design.

At necropsies of offspring on PNDs 21 and 77, weights of the brain, liver, and kidneys were measured.

Experiment 2. To evaluate the effects of developmental exposure to $MnCl_2 \cdot xH_2O$ on the serum concentrations of thyroid-related hormones and messenger RNA (mRNA) expression in the dentate gyrus, an additional $MnCl_2$ exposure study was performed (Fig. 1). Dams were randomly divided into two groups. Fifteen dams per group were treated with 0 (untreated controls) or 800 ppm Mn in the form of $MnCl_2 \cdot xH_2O$ in the MF basal diet from GD 10 to PND 21. On PND 4, the 10 dams that delivered more than 10 male offspring per group were selected to cull litters randomly, leaving 10 male offspring. Remaining dams were sacrificed under deep ether anesthesia, and the remaining offspring were sacrificed by rapid decapitation under ether anesthesia. On PND 21, all dams and 40 male offspring per group (four males per dam) were sacrificed under ether anesthesia, and blood samples were collected from the abdominal aorta. Serum was prepared and stored at −80°C to measure thyroid-stimulating hormone (TSH), triiodothyronine (T_3), and thyroxine (T_4) concentrations at Mitsubishi Chemical Medience (Tokyo, Japan). Remaining males were kept to PND 77 and subjected to blood sample collection for hormone analysis.

On PNDs 21 and 77, brains of all offspring were collected at autopsy. Five males per group (one male per dam) on PND 21 were subjected to real-time reverse transcription polymerase chain reaction (RT-PCR) assay. Remaining brains were used for other experimental purposes.

Determination of Mn and Fe Concentrations in the Cerebellum

To measure concentrations of Mn and Fe in brain tissue, frozen cerebellar tissue of dams and male offspring at PNDs 21 and 77 (dams: $n = 6$/group at PND 21; offspring: $n = 10$/group of each stage) were digested using a microwave oven (MARS5; CEM Corporation, Matthews, NC); the digested samples were analyzed using inductively coupled plasma mass spectrometry (HP-7500; Hewlett-Packard Co., Palo Alto, CA) with the monitoring mass of *m/z* as 55 for Mn and 56 for Fe. Measured Mn and Fe concentrations were normalized to total protein determined according to the micro bicinchoninic acid method (Pierce Biotechnologies, Rockford, IL) using bovine serum albumin as a standard.

Immunohistochemistry and Apoptotic Cell Detection

For immunohistochemical analysis, brains in the subgroups of male offspring sacrificed at PNDs 21 and 77 were fixed in Bouin's solution at room temperature overnight. Coronal slices embedded in paraffin at the positions of −2.2 mm from the bregma were prepared for immunohistochemical staining (3 μm in thickness).

Sections were incubated overnight at 4°C with antibodies listed in Supplementary table 1. To quench endogenous peroxidase, slides were incubated in 0.3% (vol/vol) hydrogen peroxide in absolute methanol for 30 min. Immunodetection was carried out using a VECTASTAIN Elite ABC kit (Vector Laboratories Inc., Burlingame, CA) with 3,3′-diaminobenzidine (DAB)/hydrogen peroxide (H_2O_2) as the chromogen, as previously described (Shibutani *et al.*, 2007). The sections were then counterstained with hematoxylin and coverslipped for microscopic examination.

For double staining of reelin and NeuN, a postmitotic neuron marker (Mullen *et al.*, 1992), DAB-Cobalt was used to visualize reelin and Vector Red Alkaline Phosphate Substrate Kit I (Vector Laboratories Inc.) to visualize NeuN.

For evaluation of apoptosis in the SGZ of the dentate gyrus, the terminal deoxynucleotidyl transferase dUTP nick and labeling (TUNEL) assay was applied to brain sections. Detection of apoptotic bodies was carried out using the Apop Tag *in situ* apoptosis detection kit S7100 (Millipore Corporation, Billerica, MA) according to the instructions provided by the manufacturer with DAB/H_2O_2 as the chromogen.

Morphometry of Immunolocalized Cells and Apoptotic Cells

Reelin-, NeuN-, or GAD67-positive cells distributed in the hilus of the dentate gyrus were bilaterally counted and normalized for the number per unit area of the hilar area (polymorphic layer). In the SGZ of the dentate gyrus, apoptotic bodies as detected by the TUNEL assay, proliferating cells as detected by nuclear immunoreactivity of proliferating cell nuclear antigen (PCNA), and the expression of neuronal progenitor markers including Pax6, Tbr2, NeuroD1, and TUC4 were bilaterally counted and normalized to the length of the granule cell layer measured as previously described (Saegusa *et al.*, 2010). For quantitative measurements of each immunoreactive cellular component, digital photomicrographs at 200- or 400-fold magnification were taken using a BX51 microscope (Olympus Optical Co., Ltd., Tokyo, Japan) attached to a DP70 Digital Camera System (Olympus Optical Co., Ltd.), and quantitative measurements were performed using the WinROOF image analysis software package (version 5.7, Mitani Corporation, Fukui, Japan).

Real-Time RT-PCR

For real-time RT-PCR analyses, the cerebrum of male offspring was removed at prepubertal necropsy on PND 21 ($n = 5$/group) and was fixed with methacarn solution for 8 h, then dehydrated by ice-cold absolute ethanol overnight at 4°C (Shibutani *et al.*, 2000). A coronal brain slice at the position between −2.2 and −2.8 mm from bregma was prepared, and portions of the dentate gyrus were collected using a biopsy punch (Φ1.0 mm, Kai Industries Co., Ltd., Seki, Japan) and stored in ethanol at −80°C until extraction. Total RNA was extracted with the RNeasy Mini Kit (QIAGEN, Hilden, Germany) according to the manufacturer's instructions. Analysis of mRNA levels for molecules listed in Supplementary table 2 was performed with real-time RT-PCR in the dentate gyrus tissue. *Reln*, *Lrp8*, and *Vldlr* are genes encoding reelin and its receptors (Hack *et al.*, 2007). *Gad1* encodes GAD67 (Wierońska *et al.*, 2010). *Pax6*, *Eomes* (also known as *Tbr2*), and *Dpysl3* (also known as *Tuc4*) are genes encoding neuronal-stage defining marker molecules (Breunig *et al.*, 2007; Hodge *et al.*, 2008; Knoth *et al.*, 2010). First-strand complementary DNA was synthesized from 2 μg of total RNA in the presence of dithiothreitol, deoxynucleotide triphosphates, random primers, RNaseOUT, and SuperScript III Reverse Transcriptase (Invitrogen Corporation, Carlsbad, CA) in a 20 μl total reaction mixture. Real-time PCR was performed using the Power SYBR Green PCR Master Mix (Applied Biosystems Japan Ltd., Tokyo, Japan) and the Applied Biosystems StepOnePlus Real-Time PCR System (Applied Biosystems Japan Ltd.) according to the manufacturer's protocol. The PCR primers shown in Supplementary table 2 were designed using Primer Express software (Version 3.0; Applied Biosystems Japan Ltd.). The relative differences in gene expression were calculated using threshold cycle (C_T) values that were first normalized to those of housekeeping genes, hypoxanthine-guanine phosphoribosyltransferase (*Hprt*), and glyceraldehyde 3-phosphate dehydrogenase (*Gapdh*) and then relative to a control C_T value by the $2^{-\Delta\Delta C_T}$ method (Livak and Schmittgen, 2001).

Statistical Analysis

Maternal data from experiment 1 regarding BW, food consumption, and Mn and Fe concentrations in the brain were analyzed using individual animals as the experimental unit. Data for offspring regarding the BW during the experiment, BWs, and organ weights at necropsy, Mn and Fe concentrations in the brain, immunohistochemical analysis, TUNEL assay, as well as real-time RT-PCR and serum hormonal measurements in Experiment 1 or 2 were analyzed using the litter as the experimental unit. For comparison of the numerical data between the control- and Mn-dosed groups, Bartlett's test for equal variance was used to determine whether the variance was homogenous between the groups. If the variance was homogenous, numerical data were assessed using Dunnett's test to compare between the control and each treated groups. If a significant difference in variance was observed, the Steel's test (Steel, 1959) was used instead.

In the case of data consisting of two sample groups, numerical data were assessed using the *F*-test for homogeneity of variance and Student's *t*-test was applied when the variance was homogenous between the groups using a test for equal variance. If a significant difference in variance was observed, Aspin-Welch's *t*-test was then performed.

All analyses were performed using the Excel Statistics 2008 software package (Social Survey Research Information Co. Ltd., Tokyo, Japan).

RESULTS

Maternal Data (Experiment 1)

During the gestation and lactation periods, there were no significant differences in maternal BW following $MnCl_2$ exposure (Fig. 2A). Dams in the 800 ppm group showed statistically significant decreases in food consumption from PNDs 8 to 21 (Fig. 2B). Mean daily intake of $MnCl_2$ as Mn by dams during the gestation period were 8.6 ± 0.7, 10.6 ± 1.1, 18.3 ± 7.0, and 54.2 ± 6.5 mg/kg BW/day at 0, 32, 160, and 800 ppm, respectively; during the lactation period daily intakes were 17.3 ± 4.5, 22.3 ± 1.2, 42.5 ± 8.0, and 140.9 ± 6.4 mg/kg BW/day at 0, 32, 160, and 800 ppm, respectively. $MnCl_2$ treatment did not affect the length of gestation, number of implantations in the uterus, and live births (Supplementary table 3); however, at PND 21, one dam treated with 800 ppm was found dead.

Offspring Growth and Survival (Experiment 1)

Male pups showed significant decreases in BW at 160 ppm from PNDs 21 to 70 and at 800 ppm from PNDs 17 to 63 (Fig. 3). In contrast, female pups showed no changes in BW from PNDs 2 to 77 (data not shown).

With regard to clinical signs of offspring, all male pups in the 160 and 800 ppm groups exhibited somewhat higher sensitivity against handling stimuli when compared with untreated controls. During home cage observations, both groups, particularly the 160 ppm group, showed more hyperactive and aggressive behavior, and sometimes raced around to bump into the cage wall. Until the end of Mn exposure (PND 21), one male pup for each of the 32 and 160 ppm groups and two male pups from the 800 ppm group died. After weaning, 31 male pups died through to necropsy at PND 77; however, this was not related to the dose of Mn. Six male pups died in the 32 ppm group, 14 in the 160 ppm group, and 11 from the 800 ppm group.

Offspring Body and Organ Weights at PNDs 21 and 77 (Experiment 1)

On necropsy at PND 21, BW of male pups significantly decreased following 160 ppm exposure and continued to

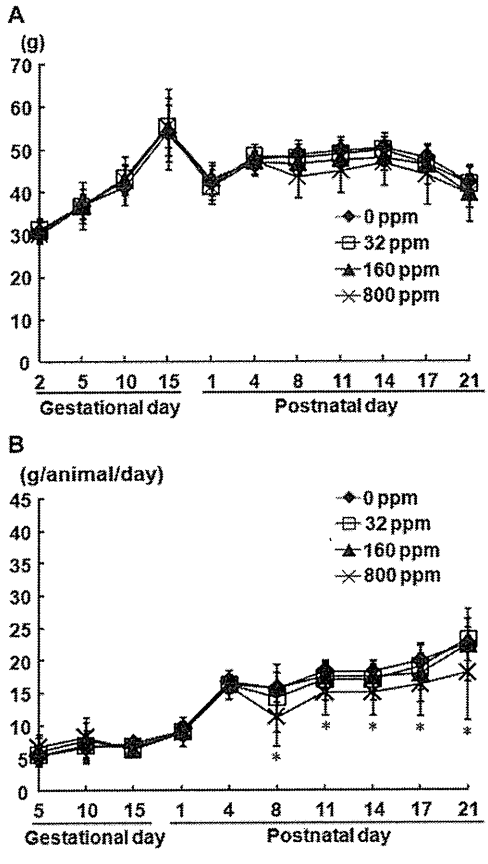

FIG. 2. BW and food consumption of dams exposed to $MnCl_2$ from GD 10 to PND 21. (A) Maternal BW. (B) Maternal food consumption. Values are expressed as the mean ± SD. *Significantly different from the untreated controls by Dunnett's test or Steel's test ($p < 0.05$).

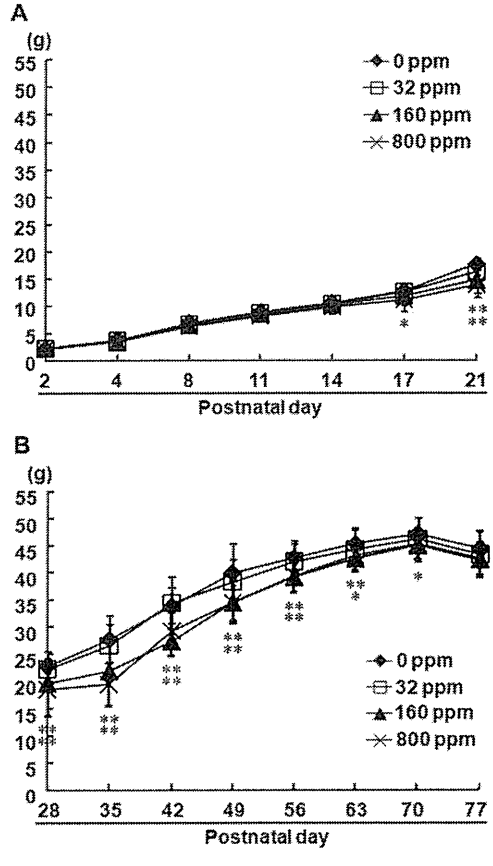

FIG. 3. BW of male offspring exposed maternally to $MnCl_2$ from GD 10 to PND 21. (A) Lactation period. (B) After lactation period. Values are expressed as the mean ± SD. * and **Significantly different from the untreated controls by Dunnett's test or Steel's test (* $p < 0.05$ and ** $p < 0.01$).

TABLE 1
Body and Organ Weights at Prepubertal and Terminal Necropsies in Male Offspring Exposed Maternally to $MnCl_2$ in the Diet From Midgestation to the End of Lactation

	Mn in diet (ppm)[a]			
	0	32	160	800
PND 21				
Number of male offspring examined	10	10	10	10
BW	17.72 ± 1.10[b]	16.23 ± 1.72	14.76 ± 2.37**	13.76 ± 2.02**
Brain (g)	0.45 ± 0.02	0.44 ± 0.03	0.43 ± 0.02	0.42 ± 0.03
g/100 g BW	2.52 ± 0.32	2.71 ± 0.23	2.96 ± 0.20**	3.11 ± 0.30**
Liver (g)	1.03 ± 0.09	0.85 ± 0.13	0.78 ± 0.22**	0.70 ± 0.10**
g/100 g BW	5.81 ± 0.25	5.24 ± 0.32*	5.16 ± 0.35**	5.11 ± 0.32**
Kidneys (g)	0.24 ± 0.02	0.22 ± 0.02	0.20 ± 0.03**	0.19 ± 0.03**
g/100 g BW	1.36 ± 0.12	1.38 ± 0.07	1.36 ± 0.08	1.40 ± 0.17
PND 77				
Number of male offspring examined	10	10	10	10
BW	44.43 ± 3.20	43.29 ± 4.26	42.22 ± 3.22	42.46 ± 2.99
Brain (g)	0.49 ± 0.02	0.50 ± 0.03	0.48 ± 0.02	0.49 ± 0.02
g/100 g BW	1.14 ± 0.11	1.14 ± 0.10	1.17 ± 0.08	1.20 ± 0.07
Liver (g)	1.81 ± 0.22	1.75 ± 0.18	1.70 ± 0.17	1.81 ± 0.15
g/100 g BW	4.15 ± 0.32	3.94 ± 0.31	4.15 ± 0.35	4.41 ± 0.33
Kidneys (g)	0.73 ± 0.14	0.70 ± 0.07	0.66 ± 0.03	0.70 ± 0.09
g/100 g BW	1.68 ± 0.25	1.59 ± 0.16	1.62 ± 0.09	1.71 ± 0.21

[a]Dietary administration of Mn was performed in the form of $MnCl_2 \cdot xH_2O$.
[b]Mean ± SD.
* and ** Significantly different from the untreated controls by Dunnett's test or Steel's test (* $p < 0.05$ and ** $p < 0.01$).

decrease in a dose-dependent manner (Table 1). The relative brain weight increased significantly from 160 ppm. With regard to liver weight, significant decreases were observed in the absolute weight from 160 ppm and in the relative weight from 32 ppm. Absolute kidney weight significantly decreased from 160 ppm. There were no significant changes in the body and organ weights following $MnCl_2$ exposure in female pups at PND 21 (data not shown).

On PND 77, there were no statistically significant differences in body, brain, liver, and kidney weights.

Serum Concentrations of Thyroid-Related Hormones in Male Offspring (Experiment 2)

Maternal $MnCl_2$ exposure at 800 ppm significantly decreased serum T_4 concentration as compared with the untreated controls, whereas serum concentrations of T_3 and TSH did not significantly change at 800 ppm (Table 2). On PND 77, serum concentrations of T_3, T_4, and TSH in offspring at 800 ppm did not show significant changes as compared with untreated controls.

Brain Concentrations of Manganese and Iron in Dams and Male Offspring (Experiment 1)

Cerebellar concentrations of Mn and Fe from dams in the $MnCl_2$ treatment groups remained unchanged at all Mn doses at PND 21. With regard to offspring, cerebellar Mn concentration showed significant dose-related increases from 32 ppm at PND 21. Although the magnitude of accumulation was rather mild, cerebellar Mn concentration increased in all dosed groups at PND 77 (Table 3). On the other hand,

TABLE 2
Serum Concentrations of Thyroid-Related Hormones

	Mn in diet (ppm)[a]	
	0	800
PND 21		
Number of offspring examined	40 (10)[b]	40 (10)
T_3 (ng/dl)	53.67 ± 6.97[c]	48.91 ± 6.85
T_4 (μg/dl)	3.62 ± 0.70	3.16 ± 0.48*
TSH (pg/ml)	11.12 ± 6.02	13.11 ± 4.09
PND 77		
Number of offspring examined	40 (10)	40 (10)
T_3 (ng/dl)	78.20 ± 10.51	80.90 ± 8.23
T_4 (μg/dl)	4.56 ± 0.56	4.87 ± 0.44
TSH (pg/ml)	48.12 ± 10.03	58.01 ± 23.02

[a]Dietary administration of Mn was performed in the form of MnCl2·xH2O.
[b]Number in parenthesis represents the total number of pooled samples: 3–4 cases/sample.
[c]Mean ± SD.
Significantly different from the untreated controls by Student's or Aspin-Welch's t-test ($p < 0.05$).

TABLE 3
Cerebellar Manganese and Iron Concentrations

	Mn in diet (ppm)[a]			
	0	32	160	800
Dams				
Number of dams examined	6	6	6	6
Mn (μg/mg protein)	0.021 ± 0.005[b]	0.022 ± 0.005	0.023 ± 0.001	0.024 ± 0.004
Fe (μg/mg protein)	0.657 ± 0.015	0.655 ± 0.012	0.654 ± 0.011	0.659 ± 0.012
Offspring				
PND 21				
Number of offspring examined	10	10	10	10
Mn (μg/mg protein)	0.022 ± 0.003	0.026 ± 0.005*	0.032 ± 0.003**	0.038 ± 0.002**
Fe (μg/mg protein)	0.452 ± 0.015	0.454 ± 0.017	0.457 ± 0.015	0.452 ± 0.012
PND 77				
Number of offspring examined	10	10	10	10
Mn (μg/mg protein)	0.013 ± 0.002	0.017 ± 0.004*	0.021 ± 0.002*	0.021 ± 0.005*
Fe (μg/mg protein)	0.545 ± 0.017	0.543 ± 0.016	0.540 ± 0.013	0.550 ± 0.018

[a]Dietary administration of Mn was performed in the form of MnCl2·xH2O.
[b]Mean ± SD.
* and ** Significantly different from the untreated controls by Dunnett's test or Steel's test (* $p < 0.05$ and ** $p < 0.01$).

cerebellar Fe concentration was unchanged in all dosed groups at both PNDs 21 and 77 in offspring.

Neuron Distribution in the Dentate Hilus of Male Offspring (Experiment 1)

In the hilus of the dentate gyrus, reelin- or GAD67-positive cells indicative of GABAergic interneurons sparsely distributed as described previously in rats (Ogawa *et al.*, 2011; Saegusa *et al.*, 2010). Statistically significant increases in the number of reelin-positive cells were observed in the 160 ppm group and increases in NeuN- and GAD67-positive cells were observed in the 800 ppm group in the hilus when compared with untreated controls at PND 21 (Figs. 4A–C). On PND 77, neurons positive for reelin or NeuN increased in the hilus at 800 ppm as compared with the untreated controls (Figs. 5A and B). GAD67 did not show any significant changes between the untreated controls and any of the $MnCl_2$-treated groups (Fig. 5C). With regard to double immunohistochemistry for reelin and NeuN, the number of neurons expressing reelin but lacking or weakly expressing NeuN increased with an Mn dose of 800 ppm at PND 21 (Fig. 4D). Neuron populations lacking reelin expression but expressing NeuN were also increased at this dose. On PND 77, a similar distribution was observed with 800 ppm Mn (Fig. 5D).

Apoptosis and Proliferating Cells in the SGZ of Male Offspring (Experiment 1)

Both TUNEL-positive apoptotic cells and PCNA-positive proliferating cells in the SGZ were sparsely observed in the SGZ on PNDs 21 and 77 (Fig. 6). Apoptotic cells significantly increased at 800 ppm on PND 21 as compared with the untreated controls (Fig. 6A); however, there was no difference with any dose of Mn at PND 77 when compared with untreated controls (Fig. 6B). The number of proliferating cells did not fluctuate with Mn at any dose on PNDs 21 and 77 as compared with the corresponding untreated controls (Figs. 6C and D).

Neuronal Progenitor Distribution in the SGZ of Male Offspring (Experiment 1)

On PND 21, the number of Pax6-, Tbr2- or NeuroD1-positive cells did not fluctuate with 800 ppm Mn (Figs. 7A–C). In contrast, a statistically significant decrease in the number of TUC4-positive cells was found at 800 ppm when compared with the untreated controls (Fig. 7D).

On PND 77, the number of progenitor cells immunoreactive for the neuronal-stage defining markers examined here decreased in the SGZ (Figs. 8A–D). TUC4-positive cells significantly increased with 800 ppm Mn treatment, whereas the number of Pax6-, Tbr2- or NeuroD1-positive cells did not fluctuate at 800 ppm.

Transcript Expression in the Dentate Gyrus of Male Offspring at PND 21 (Experiment 2)

Transcript expression levels of *Reln*, *Lrp8*, and *Gad1* after normalization with the level of *Hprt* and *Gapdh* significantly increased following exposure to 800 ppm Mn on PND 21 in comparison with the levels from untreated controls (Table 4). In contrast, transcript levels of *Dpysl3* significantly decreased at 800 ppm.

DISCUSSION

With regard to distribution changes in the neuronal progenitor cells in the SGZ, we revealed a decrease in TUC4-positive cells

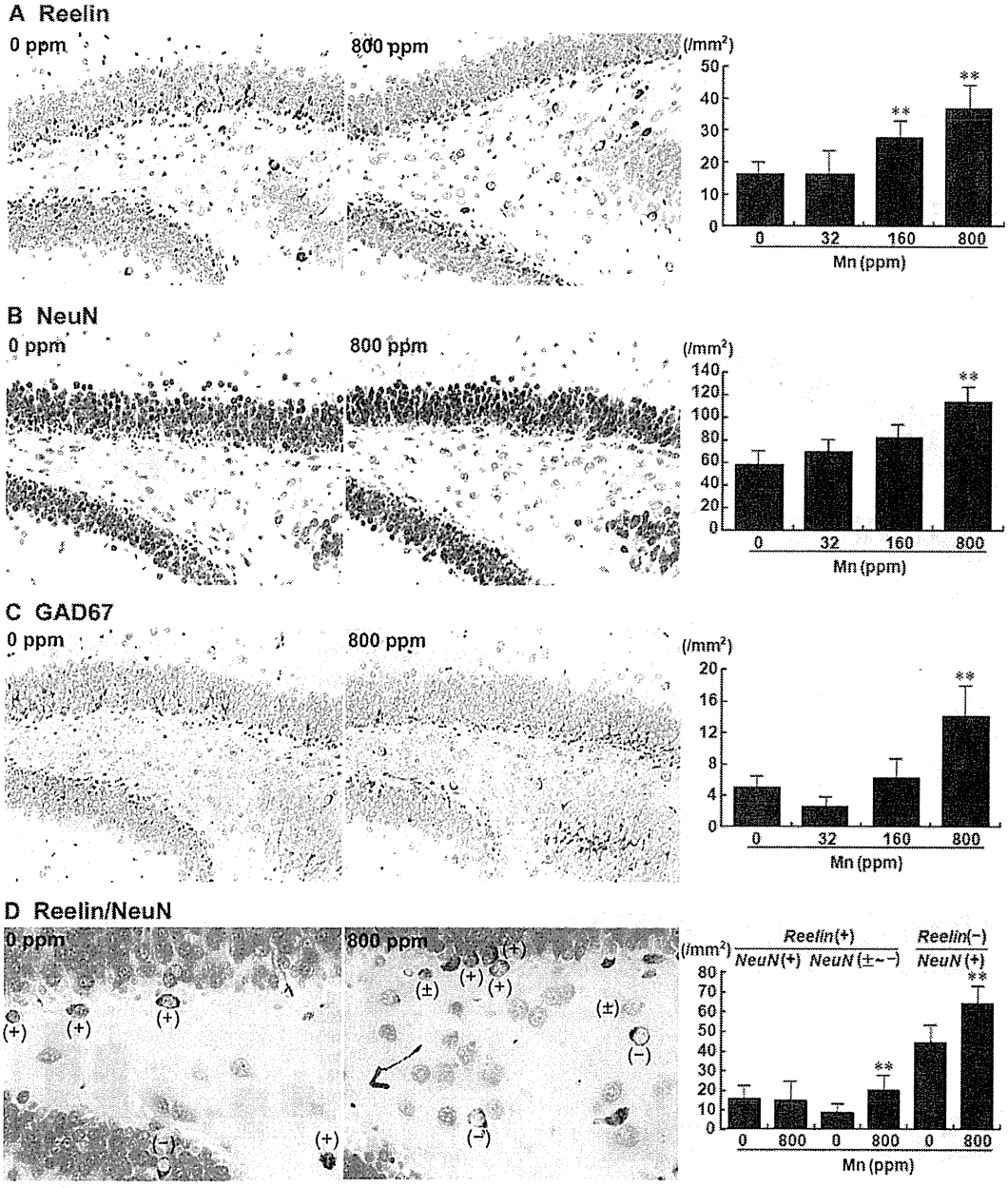

FIG. 4. Distribution of immunoreactive cells for reelin, NeuN, and GAD67 and double staining of reelin and NeuN in the dentate hilus of male offspring at PND 21 exposed maternally to $MnCl_2$ from GD 10 to PND 21. (A) Reelin. (B) NeuN. (C) GAD67. (D) Double staining of reelin (brown) and NeuN (red; for full color figures, please see online version). Representative images from 0 ppm group (left) and from 800 ppm group (right) at PND 21. (A), (B), and (C) Magnification, 200×. (D) Magnification, 400×. Graphs show the number of immunoreactive cells for each antigen/unit area (mm^2) of the hilus of the bilateral hemispheres at PND 21. Values are expressed as the mean + SD. ** Significantly different from the untreated controls by Dunnett's test or Steel's test ($p < 0.01$).

following 800 ppm Mn treatment at PND 21, whereas the distribution of progenitor cells expressing Pax6, Tbr2, and NeuroD1 was unchanged with Mn exposure. Pax6 and Tbr2 are markers for early-stage progenitor cells (Breunig *et al.*, 2007; Hodge *et al.*, 2008). In contrast, NeuroD1 is not a specific marker of neurogenesis and is expressed in cells ranging from type 2b progenitor cells to immature granule cells, with peak expression in type 3 cells (Breunig *et al.*, 2007; Hodge *et al.*, 2008; Knoth *et al.*, 2010). On the other hand, TUC4 is an early postmitotic neuronal marker of immature granule cells (Knoth *et al.*, 2010). Considering the increase in TUNEL-positive apoptotic cells in the SGZ in 800 ppm Mn-exposed offspring,

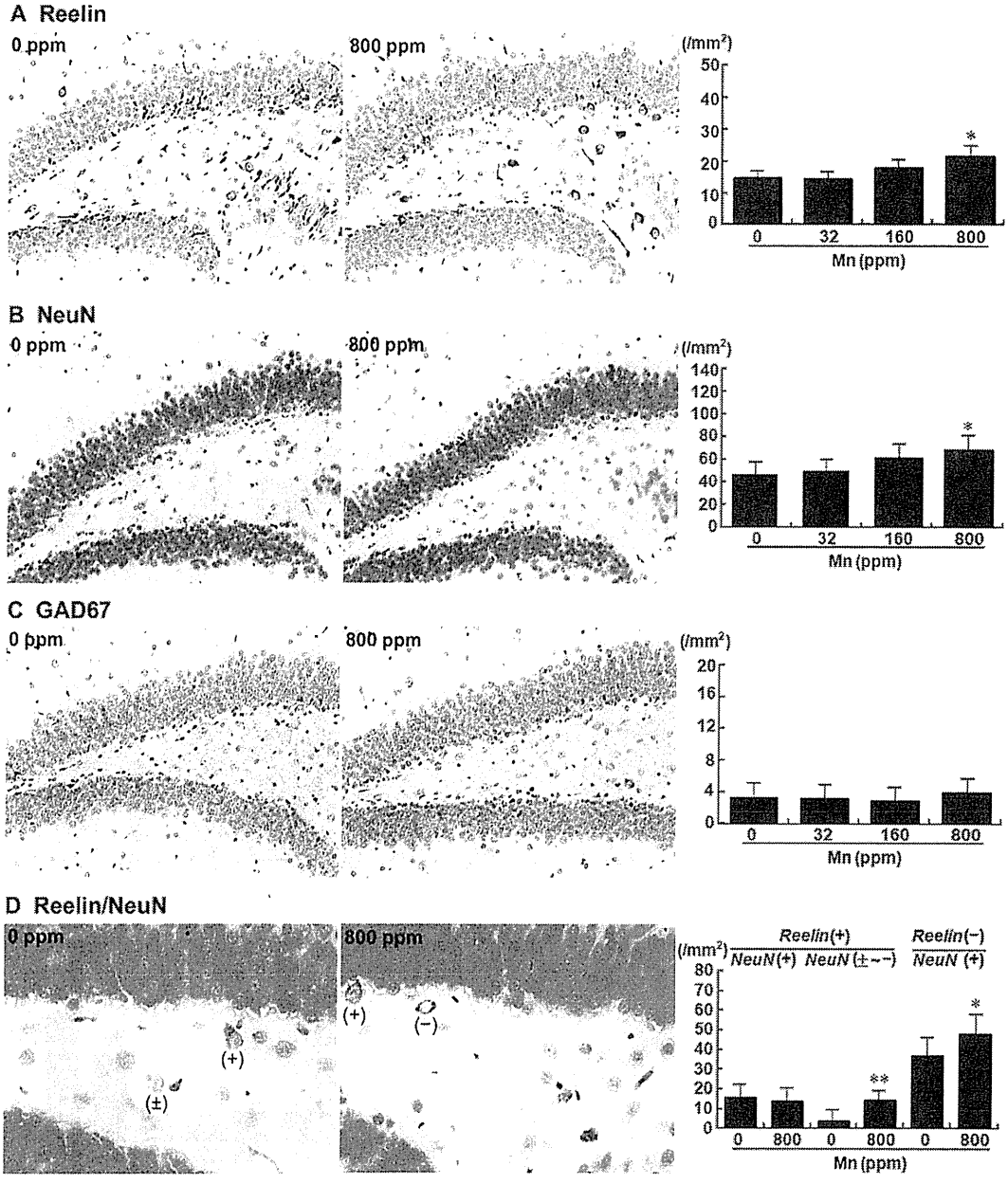

FIG. 5. Distribution of immunoreactive cells for reelin, NeuN, and GAD67 and double staining of reelin and NeuN in the dentate hilus of male offspring at PND 77 exposed maternally to $MnCl_2$ from GD 10 to PND 21. (A) Reelin. (B) NeuN. (C) GAD67. (D) Double staining of reelin (brown) and NeuN (red; for full color figures, please see online version). Representative images from 0 ppm group (left) and from 800 ppm group (right) at PND 77. (A), (B), and (C) Magnification, 200×. (D) Magnification, 400×. Graphs show the number of immunoreactive cells for each antigen/unit area (mm^2) of the hilus of the bilateral hemispheres at PND 77. Values are expressed as the mean + SD. * and ** Significantly different from the untreated controls by Dunnett's test or Steel's test (* $p < 0.05$ and ** $p < 0.01$).

developmental exposure to Mn may target immature granule cells leading to apoptosis during Mn exposure in the present study.

Similar to the developmental exposure study of antithyroid agents in rats (Saegusa *et al.*, 2010; Shibutani *et al.*, 2009), we observed a sustained increase of reelin-expressing and NeuN-lacking or weakly expressing neurons in the dentate hilus from PND 21 through to PND 77 as well as an increase of reelin-lacking and NeuN-expressing mature neurons in our $MnCl_2$-exposed cases. Reelin is a secreted extracellular matrix glycoprotein that plays a critical role in neuronal migration and positioning during brain development (D'Arcangelo *et al.*,